Physica D 448 (2023) 133728

Contents lists available at ScienceDirect

Physica D

journal homepage: www.elsevier.com/locate/physd

The N-vortex problem in a doubly periodic rectangular domain with constant background vorticity

Vikas S. Krishnamurthy [a,*], Takashi Sakajo [b]

[a] Department of Mathematics, Indian Institute of Technology Hyderabad, Kandi, Telangana 502285, India
[b] Department of Mathematics, Kyoto University, Kitashirakawa Oiwake-cho, Kyoto 606-8502, Japan

ARTICLE INFO

Article history:
Received 26 August 2022
Received in revised form 10 March 2023
Accepted 13 March 2023
Available online 21 March 2023
Communicated by Dmitry Pelinovsky

Keywords:
Point vortex dynamics
Lattice equilibria
Doubly-periodic domain
Hydrodynamic Green's function
Schottky–Klein prime function

ABSTRACT

We formulate the N point vortex problem in a doubly-periodic rectangle with a constant background vorticity using the hydrodynamic Green's function. We derive an explicit formula for the hydrodynamic Green's function and the velocities of the point vortices in terms of the Schottky–Klein prime function using a conformal mapping approach. The sum of vortex strengths can be arbitrary, and when it is zero we recover previous known results including the integrability of the two and three-vortex problems. A non-zero sum of vortex strengths leads to a constant background vorticity. We derive a Hamiltonian structure for the equations and show that the two-vortex problem is integrable, and classify all possible vortex motions. In addition, for general N, we obtain several fixed lattice equilibrium configurations including single-layered and double-layered equilibria. In the latter case, we also obtain lattice configurations with defects consisting of point vortices with inhomogeneous strengths. We find equilibria arranged in doubly-periodic rectangular and parallelogram lattices consisting of $N = 1, 2, 3, 4$ vortices per fundamental lattice.

1. Introduction

Doubly-periodic boundary conditions are commonly used in numerical studies of two-dimensional, incompressible, homogeneous and isotropic turbulent fluid flows. It is observed in such simulations that a lattice of coherent vortices dominates the flow at intermediate time scales [1,2]. To understand the interaction of these coherent vortex structures, we can approximate them as point vortices. The relation between the Euler equation, point vortices, and statistical theories of two-dimensional turbulence on the flat torus is discussed in the recent article by Geldhauser and Romito [3]. On the other hand, Feynman's (and Onsager's) prediction of the presence of quantized vortices in superfluid Helium [4] inspired Tkachenko [5] to study rotating lattice structures. The review by Newton and Chamoun [6] discusses the relation between vortex lattices and different physical phenomena such as superconductivity and superfluidity.

The equations of motion for point vortices in a doubly periodic domain have been derived by many authors. Tkachenko [5] studied rotating vortex equilibria by considering a single point vortex in a period window and studied the minimum energy vortex lattice. Benzi and Legras [7] discuss the interaction of a continuous background vorticity field with point vortices in a doubly periodic domain. O'Neil [8] derives the equations of motion for N point vortices in a period parallelogram and shows that the equations admit a Hamiltonian structure. He further gives a count of the number of relative equilibria in the case of some special domains with particular symmetry; also see O'Neil [9]. The equations of motion for N point vortices in a square doubly periodic domain were derived in terms of elementary functions by Weiss and McWilliams [10]. They also discuss the Hamiltonian structure of the equations and study the ergodicity properties of the dynamics of six-point vortices. Kilin and Artemova [11] discuss two, three and four vortex motion in a square domain using the formulas from Weiss and McWilliams [10].

In order to derive the equations of motion for the point vortices in a doubly-periodic domain, one can start with the Weierstrass zeta-function [12]. Tkachenko [5] then considers a rotating lattice, which requires the point vortex velocities to be quasi-periodic, and a special point has to be chosen as the origin of coordinates. The velocity of the point vortices is expressed in terms of the Weierstrass zeta-function by noting that this function is analytic in the period window except for a simple pole singularity. This gives the velocity field due to a single point vortex in the period window up to an arbitrary analytic function which is determined based on the requirement that the point vortex velocity is quasi-periodic. O'Neil [8] considers N point vortices in the period window with arbitrary circulations and in order to have doubly-periodic point vortex velocities, he introduces a rotating frame of reference whose angular velocity

* Corresponding author.
E-mail addresses: vikas.sk@math.iith.ac.in (V.S. Krishnamurthy), sakajo@math.kyoto-u.ac.jp (T. Sakajo).

https://doi.org/10.1016/j.physd.2023.133728
0167-2789/

is coupled to the sum of vortex strengths. The velocity field itself is then found to be doubly periodic only if the sum of the vortex strengths vanishes. Stremler and Aref [13] start with the Weierstrass zeta-function, but instead of moving into a rotating frame of reference, they assume that the sum of vortex strengths is zero, and then use a mathematical argument to obtain a doubly-periodic velocity field, and hence doubly-periodic point vortex velocities. Crowdy [14] specializes in a rectangular domain and uses a conformal mapping approach together with the Schottky–Klein prime function [15] to derive the equations of motion.

The sum of the N point vortex circulations in a period window,

$$\gamma = \sum_{k=1}^{N} \Gamma_k, \tag{1}$$

plays an important role in the theory. Stremler and Aref [13] derive the equations of motion for N point vortices with vanishing total circulation ($\gamma = 0$), and show that the three-vortex problem is integrable in this case. Stremler [16] discusses the equilibria and integrable dynamics of two and three point vortices. For the two-vortex problem with $\gamma \neq 0$, the phase portraits of an appropriate Hamiltonian are given for a few chosen lattices, as viewed from a rotating frame of reference. The dynamics of the two vortices is non-trivial but integrable when $\gamma \neq 0$, whereas only relative equilibrium solutions exist when $\gamma = 0$. Crowdy [14] considers $\gamma = 0$ in his derivation of the equations in a rectangular doubly-periodic domain. Modin and Viviani [17] discuss the integrability of the N-vortex problem in various domains using symplectic reduction theory.

In this paper, we start by considering the hydrodynamic Green's function for a doubly-periodic rectangular domain containing N point vortices with arbitrary strengths and without any constraints on their sum (Section 2). Due to the compact nature of the doubly-periodic domain, a constant background vorticity naturally arises in the Green's function on such a domain when $\gamma \neq 0$. The previous papers consider a rotating frame of reference in the general case when $\gamma \neq 0$. We simply write down the expression for this Green's function in terms of the Schottky–Klein prime function employing the same conformal mapping approach as used by Crowdy [14]. In Section 3, we use standard methods [18,19] to derive the Hamiltonian for the N vortex problem, and hence the equations of motion for the point vortices. The velocity field as well as the equations of motion for the point vortices naturally come out to be doubly periodic in all cases, even when $\gamma \neq 0$. We also discuss the integrability of the Hamiltonian system and compare our equations with previous results [8,13,14], finding that our equations are consistent with them when $\gamma = 0$. We discuss the two-vortex problem in detail in Section 4 and describe several classes of stationary lattice configurations for general N in Section 5. We summarize our results and present a discussion of future work in Section 6.

2. Hydrodynamic Green's function and stream function

Consider a doubly-periodic rectangular domain in the complex z-plane with the lattice defined by the fundamental pair of periods 2π and $-\log\rho$ for $\rho \in \mathbb{R}$, $0 < \rho < 1$. Let us denote the planar Laplacian operator by $\nabla^2 = 4\,\partial^2_{z\overline{z}}$, where an overbar denotes the complex conjugate. The Hydrodynamic Green's function $G(z, w; \overline{z}, \overline{w})$ on this domain is defined as the unique real-valued function for arguments $z, w \in \mathbb{C}$ such that the following three conditions hold.

1. $G(z, w; \overline{z}, \overline{w})$ has a logarithmic singularity at $z = w$ and satisfies the equation
$$4\,\partial^2_{z\overline{z}} G = \delta_w - \frac{1}{\text{area}(\mathcal{D}_z)}, \tag{2}$$
where δ_w is the Dirac measure and $\text{area}(\mathcal{D}_z) = -2\pi\log\rho > 0$ is the area of the fundamental domain $\mathcal{D}_z$ of the rectangular lattice. The area term in (2) is required by the Gauss divergence theorem due to the compact nature of the domain. Equivalently, this implies the existence of a function $\widehat{G}(z, w; \overline{z}, \overline{w})$ regular in $\mathcal{D}_z$:
$$\widehat{G}(z, w; \overline{z}, \overline{w}) = G(z, w; \overline{z}, \overline{w}) - \frac{1}{2\pi}\log|z - w|, \tag{3}$$
and which satisfies
$$4\,\partial^2_{z\overline{z}}\widehat{G} = \frac{1}{2\pi\log\rho}. \tag{4}$$
2. $G(z, w; \overline{z}, \overline{w})$ is doubly-periodic in both arguments, i.e.
$$G(z + 2m\pi - in\log\rho, w; \overline{z} + 2m\pi + in\log\rho, \overline{w}) = G(z, w; \overline{z}, \overline{w}), \tag{5a}$$
$$G(z, w + 2m\pi - in\log\rho; \overline{z}, \overline{w} + 2m\pi + in\log\rho) = G(z, w; \overline{z}, \overline{w}), \tag{5b}$$
for all $m, n \in \mathbb{Z}$.
3. $G(z, w; \overline{z}, \overline{w})$ satisfies the reciprocity property
$$G(z, w; \overline{z}, \overline{w}) = G(w, z; \overline{w}, \overline{z}). \tag{6}$$

Next, we introduce an auxiliary ζ-plane and a conformal map

$$z(\zeta) = -i\log\zeta \tag{7}$$

from the ζ-plane to the z-plane (see Fig. 1). The annulus $D_\zeta = \{\zeta \in \mathbb{C} : \rho < |\zeta| \leq 1, 0 \leq \arg(\zeta) < 2\pi\}$ maps to the fundamental domain $\mathcal{D}_z$. The Laplacian transforms according to

$$4\,\partial^2_{z\overline{z}} = \frac{4}{|z'(\zeta)|^2}\partial^2_{\zeta\overline{\zeta}} = 4|\zeta|^2\partial^2_{\zeta\overline{\zeta}}.$$

We denote the hydrodynamic Green's function in the annulus by $G(\zeta, \nu; \overline{\zeta}, \overline{\nu})$, where $\zeta, \nu \in \mathcal{D}_\zeta$ are the pre-images of $z, w \in \mathcal{D}_z$ respectively. $G(\zeta, \nu; \overline{\zeta}, \overline{\nu})$ satisfies the conditions

$$4\,|\zeta|^2\partial^2_{\zeta\overline{\zeta}} G = \delta_\nu + \frac{1}{2\pi\log\rho}, \tag{8a}$$
$$G(\rho^n\zeta, \rho^m\nu; \rho^n\overline{\zeta}, \rho^m\overline{\nu}) = G(\zeta, \nu; \overline{\zeta}, \overline{\nu}) \quad \text{for all } n, m \in \mathbb{Z}, \tag{8b}$$
$$\text{and} \quad G(\zeta, \nu; \overline{\zeta}, \overline{\nu}) = G(\nu, \zeta; \overline{\nu}, \overline{\zeta}). \tag{8c}$$

Note that under $\zeta \mapsto \rho^n\zeta = \rho^n e^{i2m\pi}\zeta$, we have $z \mapsto z + 2m\pi - in\log\rho$. We can define a regular function $\widehat{G}(\zeta, \nu; \overline{\zeta}, \overline{\nu})$ by

$$\widehat{G}(\zeta, \nu; \overline{\zeta}, \overline{\nu}) = G(\zeta, \nu; \overline{\zeta}, \overline{\nu}) - \frac{1}{2\pi}\log|\zeta/\nu - 1|, \tag{9}$$

where we have used

$$\log|z - w| = \log|z(\zeta) - z(\nu)| = \log|z'(\nu)(\zeta - \nu)| + O(|\zeta - \nu|) = \log|\zeta/\nu - 1| + O(1)$$

to identify the singular part of $G(\zeta, \nu; \overline{\zeta}, \overline{\nu})$. Then the regular function $\widehat{G}(\zeta, \nu; \overline{\zeta}, \overline{\nu})$ satisfies

$$4\,|\zeta|^2\partial^2_{\zeta\overline{\zeta}}\widehat{G} = \frac{1}{2\pi\log\rho}. \tag{10}$$

We now construct a hydrodynamic Green's function $G(\zeta, \nu; \overline{\zeta}, \overline{\nu})$ in terms of the Schottky–Klein prime function for an annulus. This latter function is essentially the P-function defined by (60). A function $G(\zeta, \nu; \overline{\zeta}, \overline{\nu})$ which satisfies the conditions (8) and (10) is

$$G(\zeta, \nu; \overline{\zeta}, \overline{\nu}) = \frac{1}{2\pi}\log|P(\zeta/\nu, \sqrt{\rho})| - \frac{1}{4\pi}\log|\zeta/\nu| + \frac{1}{4\pi\log\rho}(\log|\zeta/\nu|)^2. \tag{11}$$

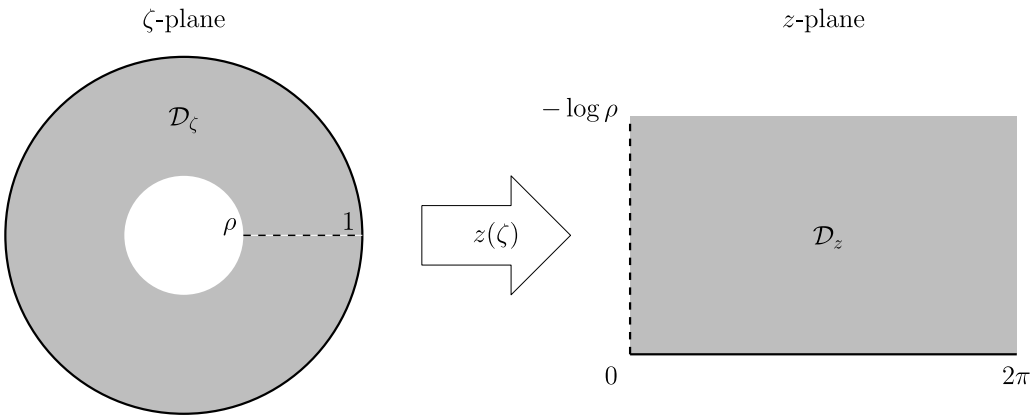

Fig. 1. The conformal map $z(\zeta) = -\mathrm{i}\log\zeta$ takes the cut annulus in the ζ-plane to the fundamental domain $\mathcal{D}_z$ in the z-plane.

The hydrodynamic Green's function is then given up to an arbitrary harmonic function by (11). Note that G depends only on the ratio ζ/ν; using (7) we have $\zeta/\nu = \mathrm{e}^{\mathrm{i}(z-w)}$, showing that the hydrodynamic Green's function (11) is independent of the definition of the origin in the z-plane. Although the Green's function has been derived for the ζ-plane, we can write it for the z-plane by simply making the substitution $\zeta/\nu = \mathrm{e}^{\mathrm{i}(z-w)}$.

From the definition of the P-function (60), it is clear that $G(\zeta,\nu;\overline{\zeta},\overline{\nu})$ has a logarithmic singularity at $\zeta=\nu$ and is regular in $\mathcal{D}_\zeta\setminus\{\nu\}$. In fact, the expression

$$\frac{1}{2\pi}\log|P(\zeta/\nu,\sqrt{\rho})| - \frac{1}{4\pi}\log|\zeta/\nu| - \frac{1}{2\pi}\log|\zeta/\nu-1|$$

is harmonic in $\mathcal{D}_\zeta$ with respect to ζ. We therefore calculate

$$4|\zeta|^2\partial^2_{\zeta\overline{\zeta}}\widehat{G} = 4|\zeta|^2\partial^2_{\zeta\overline{\zeta}}\left(\frac{1}{4\pi\log\rho}(\log|\zeta/\nu|)^2\right) = \frac{1}{2\pi\log\rho}, \quad (12)$$

showing that (10) is satisfied. The reciprocity property $G(\zeta,\nu;\overline{\zeta},\overline{\nu}) = G(\nu,\zeta;\overline{\nu},\overline{\zeta})$ is easily verified, since using (63) we have

$$\begin{aligned}
&\frac{1}{2\pi}\log|P(\nu/\zeta,\sqrt{\rho})| - \frac{1}{4\pi}\log|\nu/\zeta| \\
&\quad= \frac{1}{2\pi}\log|-\nu/\zeta\cdot P(\zeta/\nu,\sqrt{\rho})| - \frac{1}{4\pi}\log|\nu/\zeta| \\
&\quad= \frac{1}{2\pi}\log|P(\zeta/\nu,\sqrt{\rho})| - \frac{1}{4\pi}\log|\zeta/\nu|.
\end{aligned}$$

The doubly-periodic nature (8b) of $G(\zeta,\nu;\overline{\zeta},\overline{\nu})$ is confirmed in Appendix B.

2.1. The stream function

If $u-\mathrm{i}v$ is the complex velocity field for an incompressible flow in the z-plane, then a stream function $\psi(z,\overline{z})$ exists and the velocity field is defined via

$$u-\mathrm{i}v = 2\mathrm{i}\frac{\partial\psi}{\partial z}. \quad (13)$$

The vorticity $\omega(z,\overline{z})$ and the stream function are related through

$$\omega = -\nabla^2\psi. \quad (14)$$

If the flow consists of a set of N point vortices in $\mathcal{D}_z$ located at w_k with circulations Γ_k together with a constant background vorticity 2Ω, then the stream function satisfies the equation

$$\nabla^2\psi = -\sum_{k=1}^{N}\Gamma_k\,\delta_{w_k} - 2\Omega. \quad (15)$$

The double-periodicity of the flow coupled with the fact that $\mathcal{D}_z$ is a compact domain means that the area integral of the total vorticity in $\mathcal{D}_z$ vanishes. This translates into a condition between the background vorticity and the sum of point vortex strengths:

$$\Re\oint_{\partial\mathcal{D}_z}\xi\,\mathrm{d}z = 0 \implies \iint_{\mathcal{D}_z}\omega\,\mathrm{d}A = 0 \implies \Omega = \frac{\gamma}{4\pi\log\rho}. \quad (16)$$

Here $\mathrm{d}A$ is an area element in $\mathcal{D}_z$ and $\partial\mathcal{D}_z$ is the boundary of $\mathcal{D}_z$. Note that the background vorticity vanishes if and only if $\gamma=0$, i.e. the sum of point vortex strengths vanishes.

Under the conformal map (7), (15) transforms into an equation for the stream function in the ζ-plane, $\psi(\zeta,\overline{\zeta})$,

$$4|\zeta|^2\partial^2_{\zeta\overline{\zeta}}\psi = -\sum_{k=1}^{N}\Gamma_k\,\delta_{\nu_k} - 2\Omega, \quad (17)$$

where ν_k are the pre-images of the point vortices: $w_k = z(\nu_k) = -\mathrm{i}\log\nu_k$, $k=1,\dots,N$. The solution to (17) is given in terms of the hydrodynamic Green's function (11),

$$\psi(\zeta,\overline{\zeta}) = -\sum_{k=1}^{N}\Gamma_k\,G(\zeta,\nu_k;\overline{\zeta},\overline{\nu}_k). \quad (18)$$

It is easily verified by direct substitution that $\psi(\zeta,\overline{\zeta})$ satisfies (17) under the condition (16). The solution (18) is unique up to an arbitrary harmonic stream function.

The velocity field (13) transforms under (7) into

$$u-\mathrm{i}v = -2\zeta\frac{\partial\psi}{\partial\zeta}. \quad (19)$$

Substituting (18) and using (11) in (19), we find the velocity field to be

$$\begin{aligned}
u-\mathrm{i}v &= \frac{1}{2\pi}\sum_{k=1}^{N}\Gamma_k K(\zeta/\nu_k,\sqrt{\rho}) + \frac{\gamma}{2\pi}\frac{\log|\zeta/\sqrt{\rho}|}{\log\rho} \\
&\quad - \frac{1}{2\pi\log\rho}\sum_{k=1}^{N}\Gamma_k\log|\nu_k|.
\end{aligned} \quad (20)$$

We note (using (64)) that the above velocity field is loxodromic, i.e., unchanged under $\zeta\mapsto\rho\zeta$, and it is therefore doubly-periodic even when $\gamma\neq 0$.

3. Hamiltonian structure and equations of motion

The equations of motion for the point vortices in (15) admit a Hamiltonian structure with the Hamiltonian $\mathcal{H}(\boldsymbol{\nu}, \overline{\boldsymbol{\nu}})$ given by

$$\mathcal{H}(\boldsymbol{\nu}, \overline{\boldsymbol{\nu}}) = -\sum_{\substack{j,k=1\\ j<k}}^{N} \Gamma_j \Gamma_k\, G(\nu_j, \nu_k; \overline{\nu}_j, \overline{\nu}_k) - \frac{1}{2}\sum_{k=1}^{N} \Gamma_k^2\, \widehat{G}(\nu_k, \nu_k; \overline{\nu}_k, \overline{\nu}_k). \tag{21}$$

Here we use $\boldsymbol{\nu}$ as a shorthand for $\nu_1, \ldots, \nu_N$ and $\overline{\boldsymbol{\nu}}$ for $\overline{\nu}_1, \ldots, \overline{\nu}_N$. Note that due to the presence of the background vorticity, the Hamiltonian (21) is not the real part of an analytic function of $\boldsymbol{\nu}$; unlike the case of N-point vortices in an unbounded plane.

The Hamiltonian (21) is obtained using the standard procedure. That is to say, we define the N modified stream functions

$$\widehat{\psi}_j(\zeta, \overline{\zeta}) = \psi(\zeta, \overline{\zeta}) + \frac{\Gamma_j}{2\pi}\log|\zeta/\nu_j - 1|, \quad \text{for} \quad j = 1, \ldots, N; \tag{22}$$

each $\widehat{\psi}_j(\zeta, \overline{\zeta})$ is regular at $\zeta = \nu_j$. The equations of motion for the point vortices then follow from (19):

$$\begin{aligned}\frac{\mathrm{d}\overline{w}_j}{\mathrm{d}t} &= -2\zeta \frac{\partial \widehat{\psi}_j}{\partial \zeta}\bigg|_{\zeta=\nu_j} \\ &= 2\zeta \frac{\partial}{\partial \zeta}\left[\sum_{k=1}^{N}{}' \Gamma_k G(\zeta, \nu_k; \overline{\zeta}, \overline{\nu}_k) + \Gamma_j \widehat{G}(\zeta, \nu_j; \overline{\zeta}, \overline{\nu}_j)\right]\bigg|_{\zeta=\nu_j}\end{aligned} \tag{23}$$

where in the second step we have used (9) and (18), and the prime on the sum means that we omit the term $k = j$. Now, if the Hamiltonian is given in the z-plane, then the equations of motion for the point vortices are

$$\Gamma_j \frac{\mathrm{d}\overline{w}_j}{\mathrm{d}t} = 2\mathrm{i}\frac{\partial \mathcal{H}}{\partial w_j}, \quad \text{for } j = 1, \ldots, N. \tag{24}$$

Under the conformal map (7), these equations can be written in terms of variables in the ζ-plane as

$$\Gamma_j \frac{\mathrm{d}\overline{w}_j}{\mathrm{d}t} = -2\,\nu_j \frac{\partial \mathcal{H}}{\partial \nu_j}, \quad \text{for } j = 1, \ldots, N. \tag{25}$$

Substituting (21) into (25), and comparing with (23), we can verify that (21) is indeed the Hamiltonian.

The regular function of one-variable $\widehat{G}(\zeta, \zeta; \overline{\zeta}, \overline{\zeta})$ in (21) is known as the Robin function [20]. We now show that the Robin function in our case is a constant independent of its argument. Using (11) in the definition (9), along with the definition (60) of the P-function, we get

$$\begin{aligned}\widehat{G}(\zeta, \nu; \overline{\zeta}, \overline{\nu}) &= \frac{1}{2\pi}\log\left|\prod_{k=1}^{\infty}(1-\rho^k\zeta/\nu)(1-\rho^k\nu/\zeta)\right| \\ &\quad - \frac{1}{4\pi}\log|\zeta/\nu| + \frac{1}{4\pi\log\rho}(\log|\zeta/\nu|)^2,\end{aligned} \tag{26}$$

which leads to

$$\widehat{G}(\zeta, \zeta; \overline{\zeta}, \overline{\zeta}) = \frac{1}{2\pi}\log\left|\prod_{k=1}^{\infty}(1-\rho^k)^2\right|. \tag{27}$$

Substituting (21) into (25) and using (27), we get

$$\frac{\mathrm{d}\overline{w}_j}{\mathrm{d}t} = 2\sum_{k=1}^{N}{}' \Gamma_k\, \nu_j \frac{\partial}{\partial \nu_j} G(\nu_j, \nu_k; \overline{\nu}_j, \overline{\nu}_k) \quad \text{for } j = 1, \ldots, N. \tag{28}$$

Using (11), and after some algebra, we obtain the equations of motion for the point vortices:

$$\begin{aligned}\frac{\mathrm{d}\overline{w}_j}{\mathrm{d}t} &= \frac{1}{2\pi}\sum_{k=1}^{N}{}' \Gamma_k K(\nu_j/\nu_k, \sqrt{\rho}) - \frac{1}{4\pi}\sum_{k=1}^{N}{}' \Gamma_k \\ &\quad + \frac{1}{2\pi\log\rho}\sum_{k=1}^{N}{}' \Gamma_k \log|\nu_j/\nu_k| \quad \text{for } j = 1, \ldots, N.\end{aligned} \tag{29}$$

The point vortex velocities depend only on the ratios ν_j/ν_k, and thus only on the inter-vortex distances. The derivative operator $\nu_j\frac{\partial}{\partial \nu_j}$ is loxodromic, i.e., invariant under $\zeta \mapsto \rho\zeta$. This means that the velocities are loxodromic; it can also be verified directly that (29) are invariant under $\nu_k \mapsto \rho\nu_k$ and $\nu_j \mapsto \rho\nu_j$.

3.1. Conserved quantities and integrability

The Hamiltonian system (29) has three conserved quantities in general. These are the Hamiltonian (21) itself, and the two components of the linear impulse

$$Q + \mathrm{i}P = \sum_{j=1}^{N} \Gamma_j w_j = -\mathrm{i}\sum_{j=1}^{N} \Gamma_j \log \nu_j. \tag{30}$$

We show that $Q - \mathrm{i}P = \sum_{j=1}^{N} \Gamma_j \overline{w}_j$ is conserved. From (29) we have

$$\begin{aligned}\sum_{j=1}^{N} \Gamma_j \frac{\mathrm{d}\overline{w}_j}{\mathrm{d}t} &= \frac{1}{2\pi}\sum_{j,k=1}^{N}{}' \Gamma_j\Gamma_k K(\nu_j/\nu_k, \sqrt{\rho}) - \frac{1}{4\pi}\sum_{j,k=1}^{N}{}' \Gamma_j\Gamma_k \\ &\quad + \frac{1}{2\pi\log\rho}\sum_{j,k=1}^{N}{}' \Gamma_j\Gamma_k \log|\nu_j/\nu_k|.\end{aligned} \tag{31}$$

The first sum on the right hand side of (31) consists of pairs of terms like

$$\Gamma_j\Gamma_k K(\nu_j/\nu_k, \sqrt{\rho}) + \Gamma_k\Gamma_j K(\nu_k/\nu_j, \sqrt{\rho}) = \Gamma_j\Gamma_k, \tag{32}$$

where we have used (64). The last sum on the right hand side of (31) consists of pairs of terms that add up to zero:

$$\Gamma_j\Gamma_k \log|\nu_j/\nu_k| + \Gamma_k\Gamma_j \log|\nu_k/\nu_j| = 0. \tag{33}$$

Thus (31) simplifies to

$$\sum_{j=1}^{N} \Gamma_j \frac{\mathrm{d}\overline{w}_j}{\mathrm{d}t} = \frac{1}{2\pi}\sum_{\substack{j,k=1\\ j<k}}^{N} \Gamma_j\Gamma_k - \frac{1}{4\pi}\sum_{j,k=1}^{N}{}' \Gamma_j\Gamma_k = 0. \tag{34}$$

We now turn to a discussion of Liouville integrability for the N-vortex system considered here. Let the cartesian coordinates of the vortices in the z-plane be given by $w_j = x_j + \mathrm{i}y_j$. Then the canonically conjugate variables for the point vortex system are x_j and $\Gamma_j y_j$ for $j = 1, \ldots, N$. For two arbitrary functions f and g, the Poisson bracket is defined as

$$\{f, g\} = \sum_{j=1}^{N} \frac{1}{\Gamma_j}\left(\frac{\partial f}{\partial x_j}\frac{\partial g}{\partial y_j} - \frac{\partial g}{\partial x_j}\frac{\partial f}{\partial y_j}\right). \tag{35}$$

Employing the change of variables $(x_j, y_j) \mapsto (w_j, \overline{w}_j)$, this Poisson bracket can be rewritten (after some algebra) as

$$\{f, g\} = 2\mathrm{i}\sum_{j=1}^{N} \frac{1}{\Gamma_j}\left(\frac{\partial f}{\partial \overline{w}_j}\frac{\partial g}{\partial w_j} - \frac{\partial g}{\partial \overline{w}_j}\frac{\partial f}{\partial w_j}\right), \tag{36}$$

further, in terms of the coordinates ν_j in the ζ-plane (using $w_j = -\mathrm{i}\log\nu_j$) we get

$$\{f,g\} = 2\mathrm{i}\sum_{j=1}^{N}\frac{\overline{\nu}_j\nu_j}{\Gamma_j}\left(\frac{\partial f}{\partial\overline{\nu}_j}\frac{\partial g}{\partial\nu_j} - \frac{\partial g}{\partial\overline{\nu}_j}\frac{\partial f}{\partial\nu_j}\right). \tag{37}$$

The time evolution of any function f is governed by the equation

$$\frac{\mathrm{d}f}{\mathrm{d}t} = \{f,\mathcal{H}\}. \tag{38}$$

Since Q and P are constants of motion, we immediately get

$$\{Q,\mathcal{H}\} = \{P,\mathcal{H}\} = 0. \tag{39}$$

Thus we always have at least two integrals in involution, and hence the two-vortex problem is always integrable. A qualitative analysis of the two-vortex problem is provided in Section 4. When the background vorticity vanishes, i.e., $\gamma = 0$, we find that only relative equilibrium solutions are possible. But when $\gamma \neq 0$, we find relative equilibria as well as non-equilibrium solutions. We provide a complete characterization of the trajectories of the point vortices based on the Hamiltonian phase portrait for $N = 2$.

Turning to the three-vortex problem, we first note that the conserved quantities Q and P are not always in involution. From (30) we get

$$2Q = -\mathrm{i}\sum_{j=1}^{N}\Gamma_j\log\nu_j + \mathrm{i}\sum_{j=1}^{N}\Gamma_j\log\overline{\nu}_j$$
$$\text{and}\quad 2\mathrm{i}P = -\mathrm{i}\sum_{j=1}^{N}\Gamma_j\log\nu_j - \mathrm{i}\sum_{j=1}^{N}\Gamma_j\log\overline{\nu}_j,$$

from which we compute

$$\frac{\partial Q}{\partial\overline{\nu}_j} = \frac{\mathrm{i}}{2}\frac{\Gamma_j}{\overline{\nu}_j},\qquad \frac{\partial Q}{\partial\nu_j} = -\frac{\mathrm{i}}{2}\frac{\Gamma_j}{\nu_j},\qquad \frac{\partial P}{\partial\overline{\nu}_j} = -\frac{1}{2}\frac{\Gamma_j}{\overline{\nu}_j},$$
$$\frac{\partial P}{\partial\nu_j} = -\frac{1}{2}\frac{\Gamma_j}{\nu_j},$$

giving us

$$\{Q,P\} = \gamma. \tag{40}$$

For the case of $\gamma = 0$ when the background vorticity vanishes, $\{Q,P\} = 0$. Hence we have three integrals in involution, namely Q, P and $\mathcal{H}$. The three-vortex problem in this case is integrable and has been discussed in detail by Stremler and Aref [13]. In the general case when the background vorticity is non-zero, the motion may not be integrable since we do not have three integrals in involution. Kilin and Artemova [11] investigate three-vortex motion in a square domain with $\gamma \neq 0$ (as viewed from a rotating frame of reference) and provide numerical evidence that it is not integrable.

3.2. Comparison with previous results

The equations of motion (29) can be rewritten in different forms. We have

$$\sum_{k=1}^{N}{}'\,\Gamma_k = \gamma - \Gamma_j,\qquad \sum_{k=1}^{N}{}'\,\Gamma_k\log|\nu_j/\nu_k| = \sum_{k=1}^{N}\Gamma_k\log|\nu_j/\nu_k|$$
$$= \gamma\log|\nu_j| + P, \tag{41}$$

using which (29) can be written as

$$\frac{\mathrm{d}\overline{w}_j}{\mathrm{d}t} = \frac{1}{2\pi}\sum_{k=1}^{N}{}'\,\Gamma_k K(\nu_j/\nu_k,\sqrt{\rho}) + \frac{\Gamma_j}{4\pi} + \frac{\gamma}{2\pi}\frac{\log|\nu_j/\sqrt{\rho}|}{\log\rho}$$
$$+ \frac{P}{2\pi\log\rho}. \tag{42}$$

These equations take on a particularly simple form when the sum of circulations vanishes ($\gamma = 0$):

$$\frac{\mathrm{d}\overline{w}_j}{\mathrm{d}t} = \frac{1}{2\pi}\sum_{k=1}^{N}{}'\,\Gamma_k K(\nu_j/\nu_k,\sqrt{\rho}) + \frac{\Gamma_j}{4\pi} + \frac{P}{2\pi\log\rho}. \tag{43}$$

Let $\mathcal{Z}(z)$ be the Weierstrass zeta-function in the z-plane; it is related to the K-function in the ζ-plane via the identity [14]

$$K(\zeta/\nu,\sqrt{\rho}) = \frac{1}{2} - \mathrm{i}\left(\mathcal{Z}(z-w) - \frac{\mathcal{Z}(\pi)}{\pi}(z-w)\right). \tag{44}$$

Using this identity in (43), we obtain after some algebra

$$\frac{\mathrm{d}\overline{w}_j}{\mathrm{d}t} = \frac{1}{2\pi\mathrm{i}}\sum_{k=1}^{N}{}'\,\Gamma_k\,\mathcal{Z}(w_j - w_k) + \frac{\mathcal{Z}(\pi)}{2\pi^2\mathrm{i}}(Q+\mathrm{i}P) + \frac{P}{2\pi\log\rho}, \tag{45}$$

which is identical to the equation (2.19) in Stremler and Aref [13] when we remember that $\mathrm{area}(\mathcal{D}_z) = -2\pi\log\rho$. Eq. (43) is identical to the equation (19) in Crowdy [14] except for the important term $\Gamma_j/4\pi$. We have naturally obtained this term using the hydrodynamic Green's function approach. We will show later in Section 5 that the presence of this constant term captures important equilibrium configurations that are otherwise left out of the theory.

4. Two-vortex problem

In the planar (non-periodic) two-vortex problem, the only possible solutions are rotating or translating equilibria. Translating equilibria are obtained when the sum of vortex strengths is zero; rotating equilibria are obtained otherwise. Notably, no stationary equilibrium configuration of two point vortices exists. Non-trivial dynamics of the vortices is first seen in the three-vortex problem, which is integrable due to the presence of three integrals in involution, namely, the two components of linear impulse and the Hamiltonian.

When we consider the two-vortex problem in a doubly-periodic rectangular domain with vanishing background vorticity ($\gamma = 0$), we find that the vortices can form translating equilibria as well as stationary equilibria. In the presence of a background vorticity ($\gamma \neq 0$), the two vortices undergo non-trivial but integrable dynamics. A qualitative discussion of solutions is provided here, based on the Hamiltonian phase portrait for the two-vortex problem. See Stremler [16] for a previous discussion of the two-vortex problem using the Weierstrass zeta-function, including the two-vortex problem in a parallelogram domain, which is not included in our formulation.

The Hamiltonian (21) for the two-vortex problem simplifies to

$$\mathcal{H} = -\Gamma_1\Gamma_2\,G(\nu_1,\nu_2;\overline{\nu}_1,\overline{\nu}_2) + \text{const.}, \tag{46}$$

since the $\widehat{G}$'s in (21) are constants. Thus the following function of $\eta \equiv \nu_1/\nu_2$ (and $\overline{\eta}$) is a constant of motion:

$$f(\eta,\overline{\eta}) = \frac{1}{2\pi}\log|P(\eta,\sqrt{\rho})| - \frac{1}{4\pi}\log|\eta| + \frac{1}{4\pi\log\rho}(\log|\eta|)^2. \tag{47}$$

The other constant of motion, $Q + \mathrm{i}P$, can be written as (using $\nu_1 = \eta\nu_2$)

$$Q + \mathrm{i}P = -\mathrm{i}\gamma\log\nu_2 - \mathrm{i}\Gamma_1\log\eta. \tag{48}$$

If the sum of circulations vanishes, then from (48) we get $\eta = \text{const.}$, which then implies that $f = \text{const.}$; the only possible solutions are therefore relative equilibria. Since both $|\eta|$ and $\arg(\eta)$ are constant, rotating equilibria are ruled out in our model. The velocities of the point vortices are given by (29), which in this case simplify to

$$\frac{\mathrm{d}\overline{w}_1}{\mathrm{d}t} = \frac{\Gamma_2}{2\pi}K(\eta, \sqrt{\rho}) - \frac{\Gamma_2}{4\pi} + \frac{\Gamma_2}{2\pi}\frac{\log|\eta|}{\log\rho},$$
$$\frac{\mathrm{d}\overline{w}_2}{\mathrm{d}t} = \frac{\Gamma_1}{2\pi}K(1/\eta, \sqrt{\rho}) - \frac{\Gamma_1}{4\pi} + \frac{\Gamma_1}{2\pi}\frac{\log|1/\eta|}{\log\rho}.$$

Using $\gamma = \Gamma_1 + \Gamma_2 = 0$ and (64), we can show from the second equation above, that $\frac{\mathrm{d}\overline{w}_2}{\mathrm{d}t} = \frac{\mathrm{d}\overline{w}_1}{\mathrm{d}t}$ as expected from the preceding arguments. Stationary equilibria are obtained by solving for the zeros of

$$g(\eta, \overline{\eta}) := K(\eta, \sqrt{\rho}) - \frac{1}{2} + \frac{\log|\eta|}{\log\rho} = 0.$$

Although the domain of η is the annulus $\rho < |\eta| < 1/\rho$, since we have $g(\eta, \overline{\eta}) = -g(1/\eta, 1/\overline{\eta})$, we only need to consider zeros of g in the fundamental domain $\rho < |\eta| \le 1$. Further, if $\eta = \nu_1/\nu_2$ is a zero of g, then $1/\eta = \nu_2/\nu_1$ represents the same zero but with the vortices relabeled. It is readily verified using (68) that there are three solutions, $\eta = -1, \pm\sqrt{\rho}$, in the fundamental annulus. These are the only three possible solutions. For all other values of $\eta \in D_\zeta$, we obtain translating equilibria.

When there is a non-zero background vorticity, the two vortices need not necessarily be in relative equilibrium. In this case, from the conservation of linear impulse, we get

$$\frac{\mathrm{d}\overline{w}_2}{\mathrm{d}t} = -\frac{\Gamma_2}{\Gamma_1}\frac{\mathrm{d}\overline{w}_1}{\mathrm{d}t}. \tag{49}$$

The stationary equilibria for this system is the same as in the case of $\gamma = 0$, i.e., $\eta = -1, \pm\sqrt{\rho}$. It is clear from (49) that there cannot be any translating equilibria in this case since $\Gamma_1 \neq -\Gamma_2$. The Hamiltonian is given by (47), and a contour plot of the function $f(\eta, \overline{\eta})$ in the W-plane, where $W = w_1 - w_2$ and $W = -\mathrm{i}\log\eta$, is shown in Fig. 2. The stationary equilibria in the W-plane are $W = \pi$, $W = -\frac{\mathrm{i}}{2}\log\rho$, and $W = \pi - \frac{\mathrm{i}}{2}\log\rho$. Here we have chosen two values of ρ, first, $\rho = \exp(-2\pi)$ which results in a square domain (Fig. 2(a)), and second, $\rho = \exp(-3\pi/2)$ which results in a rectangular domain (Fig. 2(b)). In the case of the square domain, there is a heteroclinic separatrix connecting $W = \pi$ with $W = -\frac{\mathrm{i}}{2}\log\rho$, and $W = \pi - \frac{\mathrm{i}}{2}\log\rho$ is a center. The remaining three heteroclinic orbits seen in Fig. 2(a) are the same by the double-periodicity. Thus, there are two regimes of motion, the corresponding vortex trajectories are shown in Fig. 3.

In the case of the rectangular domain, there are three homoclinic orbits, one connecting $W = \pi$ with itself, and two connecting $W = -\frac{\mathrm{i}}{2}\log\rho$ with itself. There is also a center at $W = \pi - \frac{\mathrm{i}}{2}\log\rho$. There are thus three regimes of motion in this case, and the corresponding vortex trajectories are shown in Fig. 4.

5. Stationary equilibrium lattice configurations

A stationary equilibrium of N point vortices is a configuration in which each vortex is completely stationary. In this case, the N conditions

$$\sum_{k=1}^{N}{}' \Gamma_k K(\nu_j/\nu_k, \sqrt{\rho}) - \frac{1}{2}\sum_{k=1}^{N}{}' \Gamma_k + \frac{1}{\log\rho}\sum_{k=1}^{N}{}' \Gamma_k \log|\nu_j/\nu_k| = 0 \quad \text{for} \quad j = 1, \ldots, N, \tag{50}$$

obtained from (29), need to be satisfied. It is clear from (50) that the vortex strengths can be scaled freely. In what follows, we consider equilibria with integer vortex strengths. We find equilibria both with and without background vorticity. The sum of vortex strengths vanishes when the background vorticity is zero, i.e. $\gamma = \sum_{k=1}^{N}\Gamma_k = 0$, and the N conditions to be satisfied can be written in a simpler form using (43):

$$\sum_{k=1}^{N}{}' \Gamma_k K(\nu_j/\nu_k, \sqrt{\rho}) + \frac{\Gamma_j}{2} + \frac{P}{\log\rho} = 0 \quad \text{for} \quad j = 1, \ldots, N. \tag{51}$$

Given the vortex positions, the constant of motion P can be obtained from (30). We will use both forms of these conditions (50) and (51).

Consider N point vortices located at the vertices of a polygon in the annulus D_ζ. The vortex positions can be written as $\nu_k = r\,\mathrm{e}^{2\pi\mathrm{i}(k-1)/N}$, $1 \le k \le N$, with $\rho < r \le 1$. For $k = 1$, there is a vortex situated at $\nu_1 = r$. If $N = 2m$ is even ($m \in \mathbb{N}_{>0}$), then there is a vortex at $\nu_{m+1} = -r$ and there are $m-1$ pairs of vortices on the circle $|\zeta| = r$, appearing as complex conjugate pairs. On the other hand, if $N = 2m-1$ is odd ($m \in \mathbb{N}_{>0}$), then there are simply $m-1$ pairs of vortices on the circle $|\zeta| = r$, appearing as complex conjugate pairs. The properties (65), (66), (67), and (68) of the K-function can then be applied to prove that various configurations of vortices are in equilibrium, as we will show in this section. These properties can be applied to pairs of vortices with identical circulations and at complex conjugate positions, because then the sums in (50) and (51) consist of pairs of terms of the form $K(\zeta, \sqrt{\rho}) + K(\overline{\zeta}, \sqrt{\rho})$ with $|\zeta| = 1$, $|\zeta| = \sqrt{\rho}$ or $|\zeta| = 1/\sqrt{\rho}$.

It is important to note the difference between the shape of the domain and the lattice structure of a vortex equilibrium. The former is fixed to be a rectangular domain whereas we find both rectangular and parallelogram lattices. Increasing the number of vortices in the fundamental domain may be thought of as being equivalent to rescaling the size of the domain. Here, we present results valid for any number of vortices in a fundamental domain of fixed size, while also pointing out the particular cases which are equivalent to rescaling the domain. In our formulation, we can rescale the domain multiple times horizontally, but only once vertically.

5.1. Single-layered lattices

Consider N vortices of identical strength $+1$ arranged on a polygon in D_ζ as discussed above. The stationary conditions (50) for this case are

$$\sum_{k=1}^{N}{}' K(\nu_j/\nu_k, \sqrt{\rho}) - \frac{N-1}{2} = 0 \quad \text{for} \quad j = 1, \ldots, N. \tag{52}$$

It must be noted that the first term in (52) arises from the mutual interaction of the point vortices, whereas the second term is the contribution of the background vorticity. Due to the rotational symmetry of the polygon in D_ζ, to show that the configuration is stationary, it is sufficient to confirm that the point vortex at ν_1 is stationary.

We consider the cases when N is even and when N is odd separately. When N is even, i.e. $N = 2m$ with $m \in \mathbb{N}_{>0}$, there exist $m-1$ point vortices on both sides of the circle $|\zeta| = r$ between ν_1 and ν_{m+1}. The condition (52) for $j = 1$ is then satisfied since using $\nu_1 = r$, $\nu_{m+1} = -r$, and $\nu_{N-(k-2)} = \overline{\nu}_k$ we get

$$\sum_{k=2}^{m}\left[K(r/\nu_k, \sqrt{\rho}) + K(r/\overline{\nu}_k, \sqrt{\rho})\right] + K(-1, \sqrt{\rho}) - \frac{2m-1}{2}$$
$$= (m-1) + \frac{1}{2} - \frac{2m-1}{2} = 0,$$

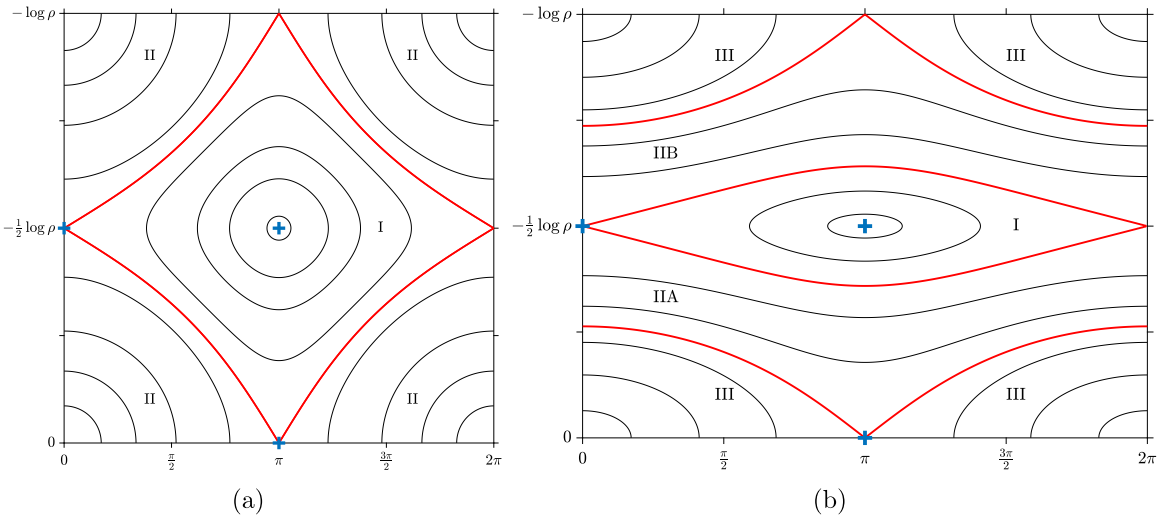

Fig. 2. Phase portraits for the Hamiltonian given by (47) in the two-vortex problem. (a) A square domain results from choosing $\rho = \exp(-2\pi)$. The red contours are the heteroclinic separatrices that divide the square into two regimes, marked I and II. The corresponding point vortex trajectories are shown in Fig. 3. (b) A rectangular domain resulting from the choice $\rho = \exp(-3\pi/2)$. There are three homoclinic separatrices, marked in red, which separate the rectangle into three domains, marked I, II, and III. Regime II is further divided into IIA and IIB, but the only difference between these two regimes is that the direction of the vortex motion is reversed between them. The corresponding point vortex trajectories are shown in Fig. 4. Note that the origin is a singularity (along with the three other corners) corresponding to $w_1 = w_2$.

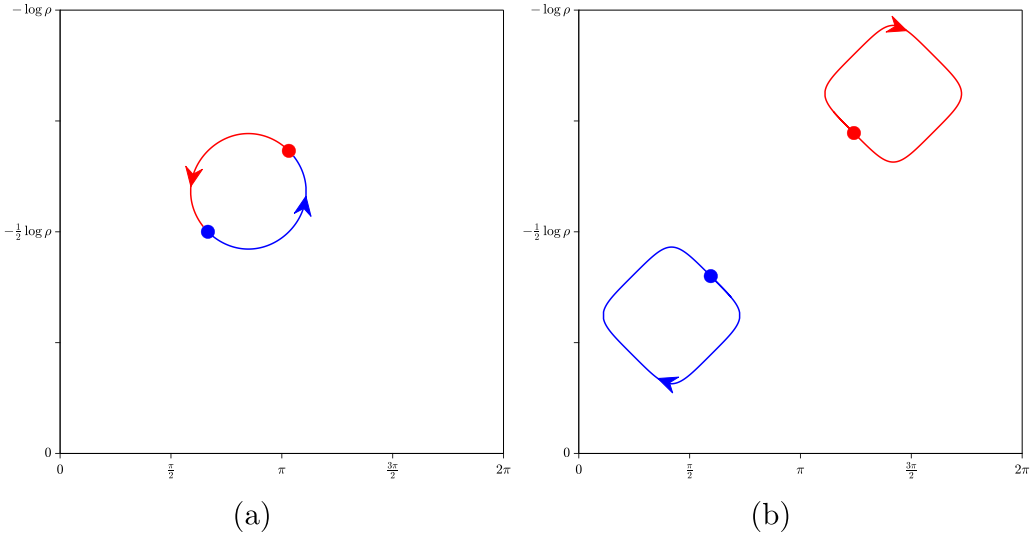

Fig. 3. Vortex trajectories in a square domain with the Hamiltonian phase portrait given by Fig. 2(a). The blue and red trajectories correspond to the two vortices, whose initial positions are marked by the disks. The arrows mark the direction of motion. (a) The two vortices chase each other in a counter-clockwise direction on the same path in the case of the trajectories of regime I. (b) The trajectories of regime II follow distinct paths, with both the vortices moving in a clockwise direction in this case.

on using (65) and (68) and keeping in mind that $|r/\nu_k| = |r/\overline{\nu}_k| = 1$. See Figure Fig. 5(a) for the case of $N = 4$. For odd $N = 2m-1$ ($m \in \mathbb{N}_{>0}$), there are $m-1$ point vortex pairs at complex conjugate positions on the circle $|\zeta| = r$, along with the vortex at $\nu_1 = r$. We can show using (65) that (52) is again satisfied for $j = 1$:

$$\sum_{k=2}^{m+1} \left[K(r/\nu_k, \sqrt{\rho}) + K(r/\overline{\nu}_k, \sqrt{\rho})\right] - (m-1)$$
$$= (m-1) - (m-1) = 0.$$

Thus the right hand side of (52) vanishes for any N, and the polygonal ring configuration is a stationary equilibrium. Since $w_k = -\mathrm{i}\log\nu_k = 2\pi(k-1)/N - \mathrm{i}\log r$, the N point vortices form a single-layered lattice configuration in D_z, equally spaced along the line $\mathrm{Im}\, z = -\log r$.

Next, consider an alternating ring of $N = 2m$ point vortices, $m \in \mathbb{N}_{>0}$, such that m vortices have strengths $+1$ and m vortices have strengths -1. Let the N vortices be equally spaced along the circle $|\zeta| = r$ in D_ζ, $\rho < r \le 1$, with alternating positive and negative strengths. That is to say, the locations and strengths of the point vortices are given by

$$\nu_{2k-1} = r\,\mathrm{e}^{2\pi\mathrm{i}(k-1)/m}, \quad \Gamma_{2k-1} = +1, \qquad \nu_{2k} = r\,\mathrm{e}^{2\pi\mathrm{i}(2k-1)/2m},$$
$$\Gamma_{2k} = -1, \qquad k = 1, \dots, m. \tag{53}$$

The total circulation vanishes, i.e., $\gamma = 0$, and hence the background vorticity also vanishes. By the rotational symmetry of the configuration in D_ζ and the invariance of the equations of motion (29) with respect to $t \mapsto -t$ and $\{\Gamma_j\} \mapsto -\{\Gamma_j\}$, it is sufficient to confirm that the point vortex at ν_1 with strength $\Gamma_1 = +1$ is stationary. The point vortices of strength, $+1$ as well

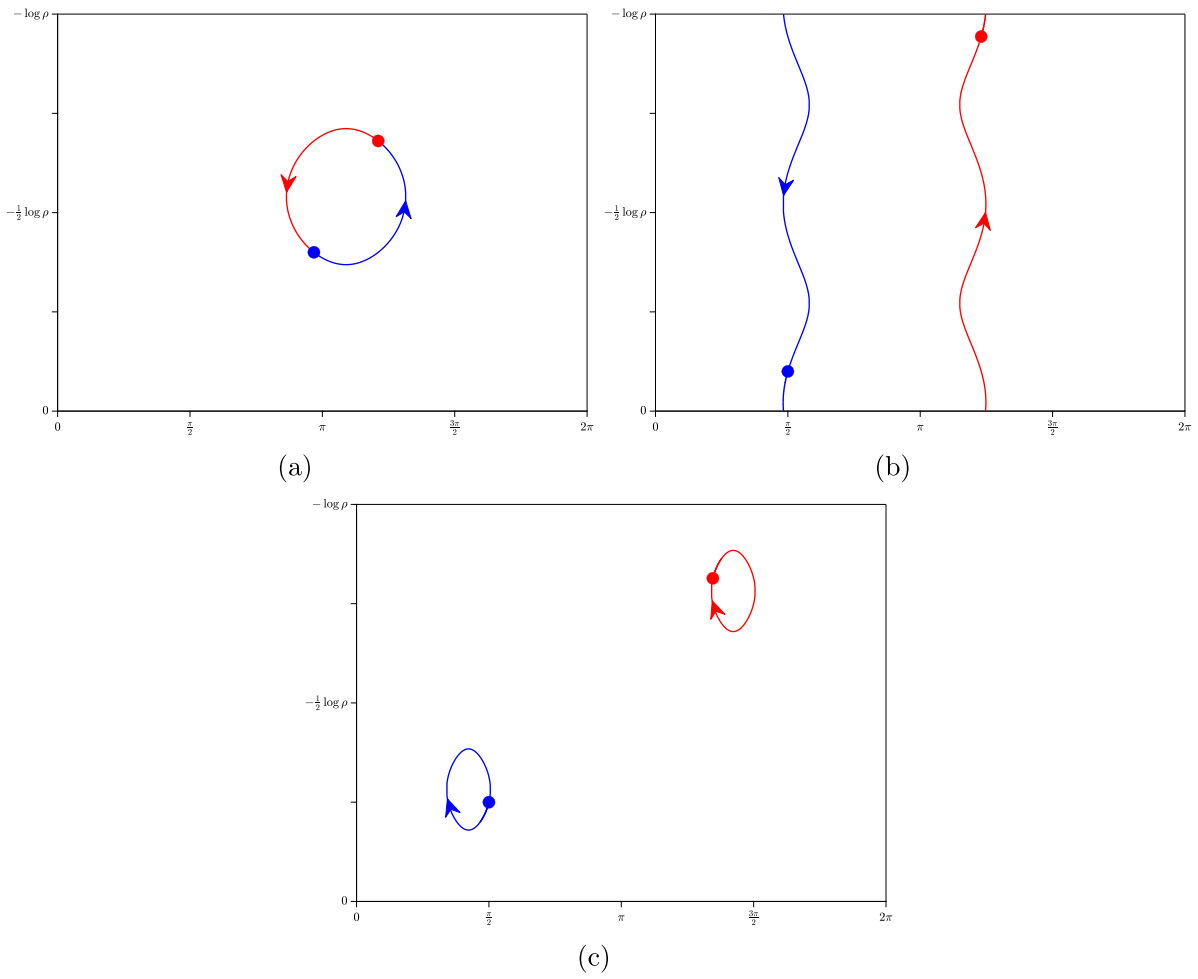

Fig. 4. Vortex trajectories in a rectangular domain with the Hamiltonian phase portrait given by Fig. 2(b). Trajectories of regimes I (panel (a)) and III (panel (c)) show similar behavior as in the case of the square domain (Fig. 3). Trajectories of regime II are shown in panel (b). In this case, the two vortices move on open paths and in opposite directions, further, there is a vortex exchange with a neighboring period window when either vortex reaches the boundary of the rectangle.

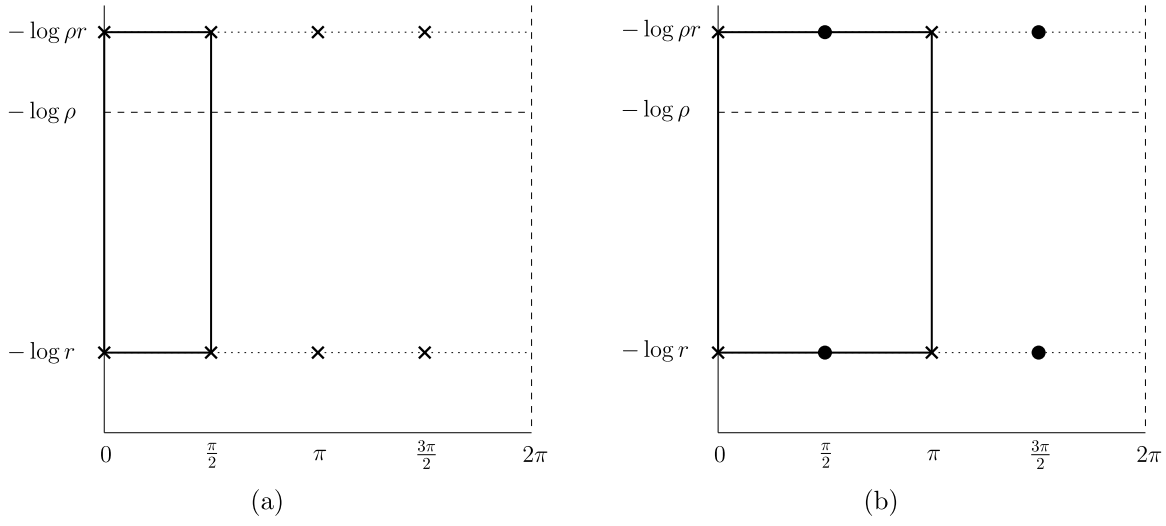

Fig. 5. Single-layered lattice equilibria of point vortices shown here for $N = 4$ in the fundamental rectangle. The cross represents a point vortex of strength $+1$, while the filled disk represents a point vortex of strength -1. (a) Homogeneous equal strengths with $\gamma \neq 0$, and (b) mixed strengths ± 1 with $\gamma = 0$. The fundamental lattice is marked by solid lines.

as -1, appear in complex conjugate pairs. When m is even, there are $\frac{m-2}{2}$ pairs of vortices off the real axis at complex conjugate positions with strength $+1$, $\frac{m}{2}$ pairs of vortices off the real axis at complex conjugate positions with strength -1, and one vortex at

$-r$ with strength $+1$. The condition (51) is satisfied since (note that $P = -\gamma \log r = 0$):

$$\frac{m-2}{2} - \frac{m}{2} + K(-1, \sqrt{\rho}) + \frac{1}{2} = 0.$$

See Figure Fig. 5(b) for the case of $m = 2$. Similarly for odd m, there are $\frac{m-1}{2}$ vortices at complex conjugate positions with strength $+1$, $\frac{m}{2}$ vortices at complex conjugate positions with strength -1, so that for the point vortex at ν_1 we have (using (51))

$$\frac{m-1}{2} - \frac{m}{2} + \frac{1}{2} = 0.$$

Hence, the configuration (53) is a fixed equilibrium. In D_z, the point vortices with the strengths ± 1 are arranged alternately along the line $\mathrm{Im}\, z = -\log r$ with the equal distance π/m between successive vortices, forming an alternating single-layered lattice.

5.2. Double-layered lattices

Let us now arrange $N = 2m$ point vortices equally along two circles in D_ζ, such that there are m point vortices with strengths $+1$ along $|\zeta| = r_1$, $\sqrt{\rho} < r_1 \le 1$, and m vortices with strengths $+1$ along $|\zeta| = r_2$, $\rho < r_2 \le \sqrt{\rho}$. We take the ratio between the two radii to be fixed according to $r_2/r_1 = \sqrt{\rho}$. The reason for choosing this value of the ratio is that $|\zeta| = \sqrt{\rho}$ is a circle of symmetry and appears in the second argument of the Schottky–Klein prime function, thus allowing us to use the properties in Appendix A to describe equilibria. The locations of these point vortices are specified by

$$\nu_{2k-1}^{(1)} = r_1 \mathrm{e}^{2\pi \mathrm{i}(k-1)/m}, \quad \Gamma_{2k-1}^{(1)} = 1, \quad \nu_{2k}^{(2)} = r_2 \mathrm{e}^{2\pi \mathrm{i}(k-1)/m}, \quad \Gamma_{2k}^{(2)} = 1, \quad k = 1, \dots, m. \tag{54}$$

Here the superscript (1) refers to vortices on the circle $|\zeta| = r_1$ and the superscript (2) refers to vortices on the circle $|\zeta| = r_2$. Due to the rotational symmetry in D_ζ, it is sufficient to show that the point vortices at $\nu_1 = r_1$ and $\nu_2 = r_2$ are stationary. Note that the two layers of vortices are unstaggered with respect to each other.

The left hand side of (50) for the vortex at ν_1 is

$$\sum_{k=1}^{m}{}' K(\nu_1/\nu_{2k-1}, \sqrt{\rho}) + \sum_{k=1}^{m} K(\nu_1/\nu_{2k}, \sqrt{\rho}) - \frac{N-1}{2} + \frac{1}{\log \rho} \sum_{k=1}^{m} \log(r_1/r_2), \tag{55}$$

and for the vortex at ν_2 is

$$\sum_{k=1}^{m} K(\nu_2/\nu_{2k-1}, \sqrt{\rho}) + \sum_{k=1}^{m}{}' K(\nu_2/\nu_{2k}, \sqrt{\rho}) - \frac{N-1}{2} + \frac{1}{\log \rho} \sum_{k=1}^{m} \log(r_2/r_1). \tag{56}$$

The arguments for equilibria are similar to those in Section 5.1. We proceed by separating the cases of even m and odd m. Let $m = 2p$, $p \in \mathbb{N}_{>0}$. For the vortex at ν_1, we find from (55)

$$(p-1) + K(-1, \sqrt{\rho}) + 2(p-1) + K(1/\sqrt{\rho}, \sqrt{\rho}) + K(-1/\sqrt{\rho}, \sqrt{\rho}) - \frac{4p-1}{2} - p = 0,$$

on using (65), (67) and (68). For the vortex at ν_2, Eq. (56) becomes

$$2p \cdot 0 + (p-1) + \frac{1}{2} - \frac{4p-1}{2} + p = 0,$$

on using (65), (66) and (68). Turning to the case of odd m, for $m = 2p-1$, $p \in \mathbb{N}_{>0}$, Eqs. (55) and (56) respectively give

$$(p-1) + 2(p-1) + 1 - \frac{4p-3}{2} - \frac{2p-1}{2} = 0 \quad \text{and} \quad (p-1) - \frac{4p-3}{2} + \frac{2p-1}{2} = 0,$$

where we have used (65)–(68). The N point vortices in configuration (54) are thus in a stationary equilibrium. They form a two-layered configuration in D_z with m vortices in one layer arranged on the line $\mathrm{Im}(z) = -\log r_1$ and m other vortices arranged on the line $\mathrm{Im}(z) = -\log r_2$, as shown in Fig. 6(a). The two layers of vortices are unstaggered with respect to each other, and successive vortices in each layer are separated by $2\pi/m$.

Let us now arrange $N = 2m$ point vortices along two circles in D_ζ but with the strength of the vortices on the second circle all equal to -1. The locations and strengths of these point vortices are

$$\nu_{2k-1}^{(1)} = r_1 \mathrm{e}^{2\pi \mathrm{i}(k-1)/m}, \quad \Gamma_{2k-1}^{(1)} = 1, \quad \nu_{2k}^{(2)} = r_2 \mathrm{e}^{2\pi \mathrm{i}(k-1)/m}, \quad \Gamma_{2k}^{(2)} = -1, \quad k = 1, \dots, m. \tag{57}$$

In this case, the sum of the vortex strengths vanishes, i.e., $\gamma = 0$. Due to the rotational symmetry in D_ζ, it is sufficient to show that the point vortices at $\nu_1 = r_1$ and $\nu_2 = r_2$ are stationary. We first calculate

$$\frac{P}{\log \rho} = -\frac{m}{\log \rho}(\log r_1 - \log r_2) = \frac{m}{2}.$$

The left hand side of condition (51) for ν_1 and ν_2 then takes the respective forms of

$$\sum_{k=1}^{m}{}' K(\nu_1/\nu_{2k-1}, \sqrt{\rho}) - \sum_{k=1}^{m} K(\nu_1/\nu_{2k}, \sqrt{\rho}) + \frac{1}{2} + \frac{m}{2},$$
$$- \sum_{k=1}^{m}{}' K(\nu_2/\nu_{2k}, \sqrt{\rho}) + \sum_{k=1}^{m} K(\nu_2/\nu_{2k-1}, \sqrt{\rho}) - \frac{1}{2} + \frac{m}{2}.$$

When $m = 2p$, $p \in \mathbb{N}_{>0}$, these sums give

$$(p-1) + \frac{1}{2} - 2(p-1) - 1 - 1 + \frac{1}{2} + p = 0 \quad \text{and} \quad -(p-1) - \frac{1}{2} - \frac{1}{2} + p = 0,$$

as desired. When $m = 2p-1$, $p \in \mathbb{N}_{>0}$, the counting gives

$$(p-1) - 2(p-1) - 1 + \frac{1}{2} + \frac{2p-1}{2} = 0 \quad \text{and} \quad -(p-1) - \frac{1}{2} + \frac{2p-1}{2} = 0,$$

again, as desired. Thus the vortices form a stationary equilibrium. The configuration (57) in D_ζ is equivalent to a double-layered lattice in D_z, in which m point vortices with strength $+1$ are equally spaced along the line $\mathrm{Im}\, z = -\log r_1$, and m point vortices with strength -1 are equally spaced along $\mathrm{Im}\, z = -\log r_2$, such that the two layers are not staggered with respect to each other, as shown in Fig. 6(b).

We can also arrange $N = 2m = 4p$ point vortices with strengths ± 1 alternately on each circle, so that we have two concentric single-layered alternating layers (see Section 5.1). The vortex strengths and positions in this case are

$$\nu_{2k-1}^{(1)} = r_1 \mathrm{e}^{2\pi \mathrm{i}(k-1)/p}, \quad \Gamma_{2k-1}^{(1)} = 1, \quad \nu_{2k}^{(1)} = r_1 \mathrm{e}^{2\pi \mathrm{i}(2k-1)/2p}, \quad \Gamma_{2k}^{(1)} = -1,$$
$$\nu_{2k-1}^{(2)} = r_2 \mathrm{e}^{2\pi \mathrm{i}(k-1)/p}, \quad \Gamma_{2k-1}^{(2)} = \pm 1, \quad \nu_{2k}^{(2)} = r_2 \mathrm{e}^{2\pi \mathrm{i}(2k-1)/2p}, \quad \Gamma_{2k}^{(2)} = \mp 1, \tag{58}$$

for $k = 1, \dots, p$. There is a vortex with strength $\Gamma_1^{(1)} = 1$ at $\nu_1^{(1)} = r_1$; we can either have a vortex of strength $\Gamma_1^{(2)} = 1$ at

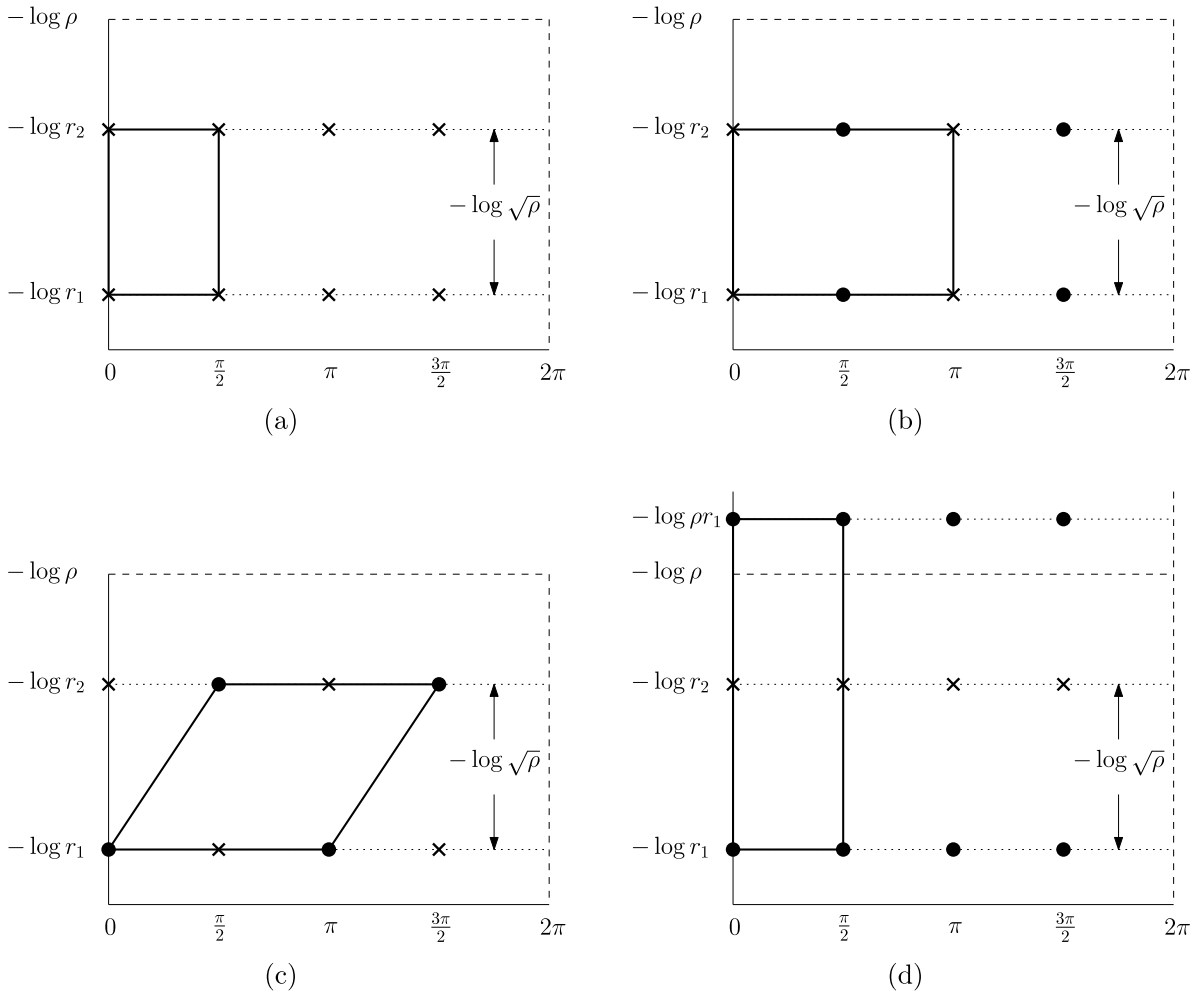

Fig. 6. Double-layered lattice equilibria with (a) homogeneous equal strengths with $\gamma \neq 0$, and (b), (c), (d) mixed strengths with $\gamma = 0$. The cross represents a point vortex of strength $+1$ while the filled disk represents a point vortex of strength -1. The fundamental lattice is marked by solid lines.

$\nu_1^{(2)} = r_2$ or a vortex of strength $\Gamma_1^{(2)} = -1$ there. The sum of vortex strengths on each circle is zero and we thus have $\gamma = 0$, which leads to $P = 0$. When $p = 2n$, $n \in \mathbb{N}_{>0}$, we count the contributions from (51) for the vortex at $\nu_1^{(1)}$ as

$$\frac{1}{2} + (-1)\cdot n + 1\cdot(n-1) + 1\cdot 2\cdot(n-1) - 1\cdot 2\cdot n + 1 + 1 + \frac{1}{2} = 0,$$

when $\Gamma_1^{(2)} = +1$, and

$$\frac{1}{2} + (-1)\cdot n + 1\cdot(n-1) - 1\cdot 2\cdot(n-1) + 1\cdot 2\cdot n - 1 - 1 + \frac{1}{2} = 0,$$

when $\Gamma_1^{(2)} = -1$. The calculations for the vortex at $\nu_1^{(2)}$ as well as for the case $p = 2n-1$, $n \in \mathbb{N}_{>0}$, are similar and we omit the details. In all these cases the conditions (51) are satisfied. Hence, the alternate double-layered lattice is a fixed equilibrium for any N and r_1, r_2 with $r_2 = \sqrt{\rho} r_1$. These configurations are equivalent to two layers of $2m$ point vortices with alternating strengths ± 1 arranged along the lines $\mathrm{Im}\, z = -\log r_1$ and $-\log r_2$ in D_z , as shown in Figs. 6(c) and (d). The fundamental lattice is a rectangular lattice in (a), (b), and (d), and a parallelogram lattice in (c). The lattices in (a) and (b) can be interpreted as the lattices in Fig. 5 but on a domain of reduced size $[0, 2\pi)\times[0, -\frac{1}{2}\log\rho)$. In fact, lattices with $N = 2m$ identical vortices on D_z can be thought of as lattices with a single vortex on the domain $[0, \pi/m) \times [0, -\frac{1}{2}\log\rho)$. We thus see that the fundamental lattice in (a) contains one point vortex. The fundamental lattices in (b), (c), and (d) contain two point vortices; these are the three two-vortex equilibria obtained in Section 4 for the case $\gamma = 0$.

We also consider staggered double-layered lattices in each of the four types of equilibria studied above. If each layer in D_z contains m point vortices, and further if the stagger between the two layers is π/m, then we can show that the configuration is an equilibrium configuration. In the examples shown in Figs. 7(a) and (b), the fundamental lattices are parallelogram lattices, whereas in Figs. 7(c) and (d), they are taken to be rectangular lattices containing interior vortices. In these examples, there is one vortex in (a), and two vortices of equal and opposite sign in (b) and (d), contained in the fundamental domain. These two-vortex equilibria are discussed in Section 4 (the case $\gamma = 0$). The example in (c) consists of a four-vortex equilibrium in the fundamental domain.

5.3. Double-layered lattices with defects

Consider the following configuration consisting of $N = 3m$, $m \in \mathbb{N}_{>0}$ point vortices in D_ζ.

$$\begin{aligned} \nu_k^{(1)} &= r_1 e^{2\pi i(k-1)/2m}, \quad \Gamma_k^{(1)} = 1, \quad k = 1, \ldots, 2\,m, \\ \nu_k^{(2)} &= r_2 e^{2\pi i(k-1)/m}, \quad \Gamma_k^{(2)} = -2, \quad k = 1, \ldots, m, \end{aligned} \tag{59}$$

where $\rho < r_2 \le \sqrt{\rho}$, $\sqrt{\rho} < r_1 \le 1$ with $r_2 = \sqrt{\rho} r_1$. In the fundamental domain D_z, $2m$ point vortices with strength $+1$ each are arranged along the line $\mathrm{Im} z = -\log r_1$, with successive vortices

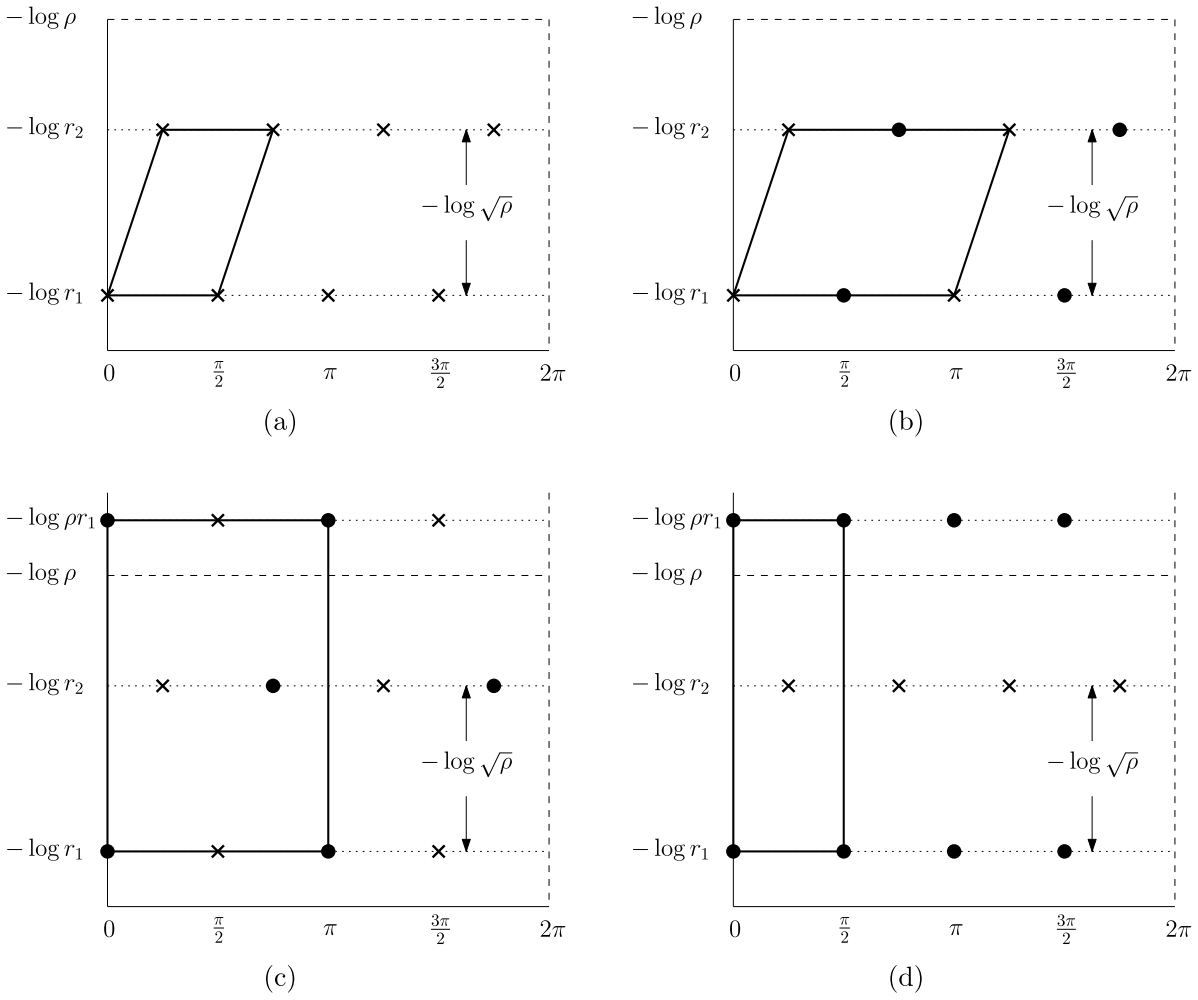

Fig. 7. Double-layered staggered lattice equilibria with (a) homogeneous equal strengths ($\gamma \neq 0$), and (b), (c), (d) mixed strengths ($\gamma = 0$). The cross represents a point vortex of strength $+1$ while the filled disk represents a point vortex of strength -1. The fundamental lattice is marked by solid lines.

separated by π/m, whereas m point vortices with strength -2 each are arranged along the line $\mathrm{Im} z = -\log r_2$, with successive vortices separated by $2\pi/m$. The resulting configuration is a double-layered lattice structure but with point vortices absent from the sites $\zeta = r_2 e^{2\pi i(2k-1)/2m}$ for $k = 1, \ldots, m$ along the line $\mathrm{Im} z = -\log r_2$, in other words the lattice structure has periodic "defects".

Since the total circulation vanishes, the vortices need to satisfy (51) to be in equilibrium. We can calculate the last term in (51) to be

$$\frac{P}{\log\rho} = -\frac{1}{\log\rho}(2m\log r_1 - 2m\log r_2) = m.$$

Consider the vortex at $\nu_1 = r_1$. There are always an even number of vortices on $|\zeta| = r_1$, so that the contribution to the left hand side of (51) from these vortices is $\frac{1}{2} + (m-1)$. The remaining vortices contribute $-4\cdot(p-1)-2-2$ when $m = 2p$, and $-4\cdot(p-1)-2$ when $m = 2p-1$, $p \in \mathbb{N}_{>0}$. Accordingly, Eq. (51) gives

$$\frac{1}{2} + (2p-1) - 4\cdot(p-1) - 2 - 2 + \frac{1}{2} + 2p = 0$$

when m is even, and when m is odd we get

$$\frac{1}{2} + (2p-2) - 4\cdot(p-1) - 2 + \frac{1}{2} + 2p - 1 = 0,$$

which shows that the vortex at $\nu_1^{(1)}$ is stationary. A similar calculation shows that the vortex at $\nu_1^{(2)}$ is also stationary. By rotational symmetry in D_ζ, the double-layered lattice with defects at $\zeta = r_2 e^{2\pi i(2k-1)/2m}$, $k = 1, \ldots, m$ is a fixed equilibrium. An example configuration is shown in Fig. 8(a). The fundamental lattice here is a face-centered rectangular lattice, in which two vortices of equal strengths $+1$ and one vortex of strength -2 are contained.

We can also consider two other configurations of $N = 3m$ vortices in a double-layered configuration with defects. These configurations consist of an alternating layer of vortices of strength 1 and -2 on $|\zeta| = r_1$ and a layer with defects on $|\zeta| = r_2$. The layer with defects can be either staggered or unstaggered. The vortex locations and circulations for the two configurations are

$$\nu_{2k-1}^{(1)} = r_1 e^{2\pi i(k-1)/m}, \quad \Gamma_k^{(1)} = 1, \quad \nu_{2k}^{(1)} = r_1 e^{2\pi i(2k-1)/2m}, \quad \Gamma_k^{(1)} = -2,$$
$$\nu_k^{(2)} = r_2 e^{2\pi i(k-1)/m}, \quad \Gamma_k^{(2)} = 1, \qquad k = 1, \ldots, m,$$

and

$$\nu_{2k-1}^{(1)} = r_1 e^{2\pi i(k-1)/m}, \quad \Gamma_k^{(1)} = 2\pi, \quad \nu_{2k}^{(1)} = r_1 e^{2\pi i(2k-1)/2m}, \quad \Gamma_k^{(1)} = -2,$$
$$\nu_k^{(2)} = r_2 e^{2\pi i k/m}, \quad \Gamma_k^{(2)} = 1, \qquad k = 1, \ldots, m.$$

where $\rho < r_2 \leq \sqrt{\rho} < r_1 \leq 1$ with $r_2 = \sqrt{\rho} r_1$. In both cases, the total circulation vanishes. The proof that these configurations are equilibria has similar counting as before and we omit the details here. Example configurations are shown in Figs. 8(b) and (c) with the fundamental lattices being face-centered and face-

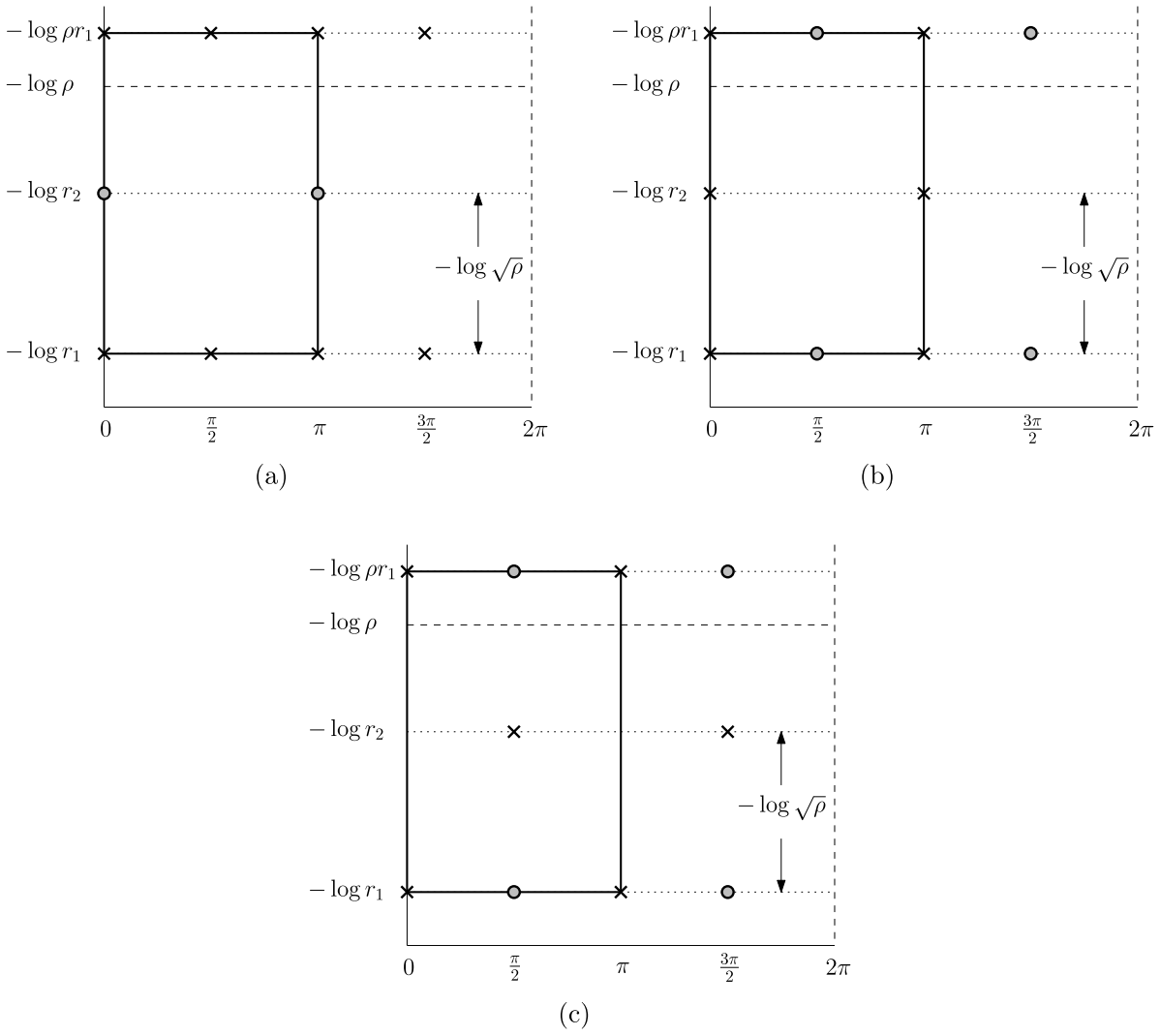

Fig. 8. Double-layered lattice equilibria with defects and $\gamma = 0$. A point vortex with strength $+1$ is represented by a cross, and a point vortex with strength -2 is represented by a gray disk. The fundamental lattice is marked by solid lines.

and body-centered rectangular lattices respectively. Each of these is an equilibrium consisting of three vortices in the fundamental lattice with $\gamma = 0$.

6. Summary and future directions

We have derived the equations of motion for N point vortices in a rectangular doubly-periodic domain using the hydrodynamic Green's function. All of our equations are found to be consistent with previously known results in the literature when the sum of vortex strengths vanishes. The effect of a non-zero-sum of vortex strengths appears as a constant background vorticity in our theory. Previous authors [5,8] have invoked a rotating frame of reference in which the background vorticity term disappears. In our formulation there is no preferred origin and hence a lack of rotational symmetry in the physical plane, which in particular means that rigidly rotating lattice equilibria are not covered here. We have explicitly shown that the two-vortex problem is Liouville integrable for any sum of vortex strengths, and provide a classification of dynamics based on the Hamiltonian phase portrait. We also show that the three-vortex problem is Liouville integrable when the sum of vortex strengths is zero, but it may not be integrable when the sum of vortex strengths is non-zero. We find several equilibrium lattice structures for arbitrary N, including lattices with defects and inhomogeneous vortex strengths. Although the conformal mapping we use maps the annulus to a rectangular domain, the lattice structure need not be rectangular and we find parallelogram as well as face and body centered rectangular lattices. The lattices for larger N can be rescaled and hence interpreted as lattices with $N = 1, 2, 3, 4$ in a domain of reduced size. In particular, the $N = 4$ example that we present in Fig. 7(c) appears to be new. The lattice equilibria obtained here are all fixed equilibria.

Vortex equilibria and dynamics on a curved torus can be considered by means of a stereographic projection to an annulus where a Green's function can be constructed [21]. In order to obtain the hydrodynamic Green's function which satisfies the reciprocity condition on this domain, it is found that an additional term is required [22]. A numerical method is used to obtain relative equilibria on a curved torus with a constant background vorticity in Sakajo [23]. The hydrodynamic Green's function obtained in the present paper differs from all these preceding Green's functions.

We can consider a non-constant background vorticity in the doubly-periodic domain. Recent work suggests that a Liouville-type vorticity, which is exponentially related to the stream function, is a good candidate for such a background vorticity. Large

families of solutions called 'Liouville chains' have been constructed recently in the case of the unbounded plane [24,25]. A one-way interaction model with point vortices in a Liouville-type background on a curved torus was studied recently by Sakajo [23],Sakajo and Krishnamurthy [26]. To the best of the authors' knowledge, no previous work has considered a Liouville-type equation in a doubly-periodic domain, although there are results on vortices described by the sinh-Poisson equation [27].

O'Neil [28] numerically investigated the collapse of point vortex lattices in a rotating frame of reference. Although there are several papers dealing with finite-time collapse in the unbounded plane, collapse in a doubly-periodic domain is much less studied. The equations of motion derived here could be used to study collapsing orbits of point vortices with a constant background vorticity. Another future direction is to consider the dynamics of vortex patches in the doubly-periodic domain and to derive the contour dynamics for the Euler equations making use of the explicit Green's function available here [29,30].

Declaration of competing interest

The authors declare the following financial interests/personal relationships which may be considered as potential competing interests: Takashi Sakajo reports financial support was provided by Japan Society for the Promotion of Science.

Data availability

No data was used for the research described in the article.

Acknowledgment

This work is supported by JSPS, Japan Kakenhi(B) #18H01136T.

Appendix A. Schottky–Klein prime functions

The Schottky–Klein prime function is a special function defined on multiply-connected circular domains [15]. The prime function defined on the annulus $D_\zeta = \{\zeta \in \mathbb{C} \,|\, \rho < |\zeta| \le 1\}$, is essentially the P-function given by the infinite product

$$P(\zeta, \sqrt{\rho}) = (1-\zeta)\prod_{k=1}^{\infty}(1-\rho^k\zeta)(1-\rho^k/\zeta). \tag{60}$$

Note that $P(\zeta, \sqrt{\rho})$ has a simple zero at $\zeta = 1$ in D_ζ. The K-function defined in terms of the logarithmic derivative of $P(\zeta, \sqrt{\rho})$ is

$$K(\zeta, \sqrt{\rho}) = \frac{\zeta P'(\zeta, \sqrt{\rho})}{P(\zeta, \sqrt{\rho})}. \tag{61}$$

Here, the prime denotes the derivative with respect to the first argument, thus $P'(\zeta, \sqrt{\rho}) = \frac{\mathrm{d}P(\zeta, \sqrt{\rho})}{\mathrm{d}\zeta}$. We can deduce the infinite series formula

$$\begin{aligned} K(\zeta, \sqrt{\rho}) &= \frac{\zeta}{\zeta-1} + \sum_{k=1}^{\infty}\left(\frac{-\rho^k\zeta}{1-\rho^k\zeta} + \frac{\rho^k/\zeta}{1-\rho^k/\zeta}\right) \\ &= \frac{1}{\zeta-1} + O(1) \quad \text{as } \zeta \to 1, \end{aligned} \tag{62}$$

showing that $K(\zeta, \sqrt{\rho})$ has a simple pole singularity at $\zeta = 1$.

The P-function satisfies the following properties

$$\begin{aligned} &P(\rho\zeta, \sqrt{\rho}) = -(1/\zeta)P(\zeta, \sqrt{\rho}) \\ &\text{and} \quad P(1/\zeta, \sqrt{\rho}) = -(1/\zeta)P(\zeta, \sqrt{\rho}). \end{aligned} \tag{63}$$

It can be verified from the above definitions that the K-function satisfies the useful identity:

$$K(\rho\zeta, \sqrt{\rho}) = K(\zeta, \sqrt{\rho}) - 1 = -K(1/\zeta, \sqrt{\rho}). \tag{64}$$

A consequence of the second equality in (64) is

$$K(\zeta, \sqrt{\rho}) + K(\overline{\zeta}, \sqrt{\rho}) = 1 \quad \text{on} \quad |\zeta| = 1, \tag{65}$$

since on $|\zeta| = 1$ with $\overline{\zeta} = 1/\zeta$. We also have

$$K(\zeta, \sqrt{\rho}) + K(\overline{\zeta}, \sqrt{\rho}) = 0 \quad \text{on} \quad |\zeta| = \sqrt{\rho}, \tag{66}$$

$$K(\zeta, \sqrt{\rho}) + K(\overline{\zeta}, \sqrt{\rho}) = 2 \quad \text{on} \quad |\zeta| = 1/\sqrt{\rho}. \tag{67}$$

To prove (66), note that Eq. (64) can also be written as $K(\rho/\zeta, \sqrt{\rho}) = -K(\zeta, \sqrt{\rho})$. Similarly, it can also be written as $K(\rho^2\zeta, \sqrt{\rho}) = K(\rho\zeta, \sqrt{\rho}) - 1 = K(\zeta, \sqrt{\rho}) - 2 = -K(1/\rho\zeta, \sqrt{\rho})$, which leads to (67). Setting $\zeta = 1$ in (65), $\zeta = \pm\sqrt{\rho}$ in (66), and $\zeta = \pm 1/\sqrt{\rho}$ in (67) gives us the useful formulae:

$$\begin{aligned} &K(-1, \sqrt{\rho}) = 1/2, \quad K(\pm\sqrt{\rho}, \sqrt{\rho}) = 0, \\ &\text{and} \quad K(\pm 1/\sqrt{\rho}, \sqrt{\rho}) = 1. \end{aligned} \tag{68}$$

We finally mention that for numerical computations, the above special functions are all evaluated using a rapidly convergent Laurent series for the prime function in the annulus, see Crowdy [15,31] for details.

Appendix B. Double periodicity of the Green function $G(\zeta, \nu; \overline{\zeta}, \overline{\nu})$

We first check the following formulae of $P(\zeta, \sqrt{\rho})$ for $n \ge 1$ by induction.

$$\begin{aligned} P(\rho^n\zeta, \sqrt{\rho}) &= (-1)^n \frac{1}{\rho^{n(n-1)/2}} \frac{1}{\zeta^n} P(\zeta, \sqrt{\rho}), \quad P(\zeta/\rho^n, \sqrt{\rho}) \\ &= (-1)^n \frac{\zeta^n}{\rho^{n(n+1)/2}} P(\zeta, \sqrt{\rho}). \end{aligned}$$

For $n = 1$, from the definition, it is easy to see that

$$\begin{aligned} P(\rho\zeta, \sqrt{\rho}) &= (1-\rho\zeta)\prod_{n\ge 1}(1-\rho^{n+1}\zeta)(1-\rho^{n-1}(1/\zeta)) \\ &= \frac{(1-1/\zeta)}{(1-\zeta)} P(\zeta, \sqrt{\rho}) = -\frac{P(\zeta, \sqrt{\rho})}{\zeta}, \\ P(\zeta/\rho, \sqrt{\rho}) &= (1-\zeta/\rho)\prod_{n\ge 1}(1-\rho^{n-1}\zeta)(1-\rho^{n+1}(1/\zeta)) \\ &= -\frac{\zeta}{\rho} P(\zeta, \sqrt{\rho}). \end{aligned}$$

Assume that they hold for $n-1$. Then we have

$$\begin{aligned} P(\rho\cdot(\rho^{n-1}\zeta), \sqrt{\rho}) &= -\frac{1}{\rho^{n-1}\zeta} P(\rho^{n-1}\zeta, \sqrt{\rho}) \\ &= -\frac{1}{\rho^{n-1}\zeta} \cdot (-1)^{n-1} \frac{1}{\rho^{(n-1)(n-2)/2}} \frac{1}{\zeta^{n-1}} P(\zeta, \sqrt{\rho}) \\ &= (-1)^n \frac{1}{\rho^{n(n-1)/2}} \frac{1}{\zeta^n} P(\zeta), \\ P\left(\frac{1}{\rho}\cdot\left(\frac{\zeta}{\rho^{n-1}}\right), \sqrt{\rho}\right) &= -\frac{\zeta}{\rho^n} P\left(\frac{\zeta}{\rho^{n-1}}, \sqrt{\rho}\right) \\ &= -\frac{\zeta}{\rho^n} \cdot (-1)^{n-1} \frac{\zeta^{n-1}}{\rho^{n(n-1)/2}} P(\zeta, \sqrt{\rho}) \\ &= (-1)^n \frac{\zeta^n}{\rho^{n(n+1)/2}} P(\zeta, \sqrt{\rho}). \end{aligned}$$

They are expressed in one formula for $n \in \mathbb{Z}$.

$$P(\rho^n\zeta, \sqrt{\rho}) = (-1)^n \frac{1}{\rho^{n(n-1)/2}} \frac{1}{\zeta^n} P(\zeta, \sqrt{\rho}). \tag{69}$$

For convenience, we introduce a parameter $\mathcal{A} = -\frac{1}{2\pi}\log\rho$ in what follows. It follows from (69) that we obtain

$$\begin{aligned}
&\frac{1}{2\pi}\log\left|P\left(\rho^n\frac{\zeta}{\nu},\sqrt{\rho}\right)\right| \\
&= \frac{1}{2\pi}\log\left|(-1)^n\frac{1}{\rho^{n(n-1)/2}}\left(\frac{\nu}{\zeta}\right)^n P\left(\frac{\zeta}{\nu},\sqrt{\rho}\right)\right| \\
&= \frac{n(n-1)}{2}\mathcal{A} - \frac{n}{2\pi}\log\left|\frac{\zeta}{\nu}\right| + \frac{1}{2\pi}\log\left|P\left(\frac{\zeta}{\nu},\sqrt{\rho}\right)\right|. \qquad (70)
\end{aligned}$$

For $n\in\mathbb{Z}$, it is easy to confirm that

$$\frac{1}{4\pi}\log\left|\rho^n\frac{\zeta}{\nu}\right| = -\frac{n}{2}\mathcal{A} + \frac{1}{4\pi}\log\left|\frac{\zeta}{\nu}\right|, \qquad (71)$$

$$\begin{aligned}
\frac{1}{4\pi\log\rho}\left(\log\left|\rho^n\frac{\zeta}{\nu}\right|\right)^2 &= -\frac{1}{8\pi^2\mathcal{A}}\left(-2\pi n\mathcal{A} + \log\left|\frac{\zeta}{\nu}\right|\right)^2 \\
&= -\frac{1}{8\pi^2\mathcal{A}}\left(4\pi^2n^2\mathcal{A}^2 - 4\pi n\mathcal{A}\log\left|\frac{\zeta}{\nu}\right| \right.\\
&\quad \left. + \left(\log\left|\frac{\zeta}{\nu}\right|\right)^2\right) \\
&= -\frac{n^2}{2}\mathcal{A} + \frac{n}{2\pi}\log\left|\frac{\zeta}{\nu}\right| \\
&\quad + \frac{1}{4\pi\log\rho}\left(\log\left|\frac{\zeta}{\nu}\right|\right)^2. \qquad (72)
\end{aligned}$$

Hence, owing to (69), (71) and (72) yield, we have the doubly-periodic nature (8b). For $n,m\in\mathbb{Z}$ and $\zeta,\nu\in D_\zeta$,

$$\begin{aligned}
&G(\rho^n\zeta,\rho^m\nu;\rho^n\overline{\zeta},\rho^m\overline{\nu}) = \frac{1}{2\pi}\log\left|P\left(\rho^{n-m}\frac{\zeta}{\nu},\sqrt{\rho}\right)\right| \\
&\quad - \frac{1}{4\pi}\log\left|\rho^{n-m}\frac{\zeta}{\nu}\right| + \frac{1}{4\pi\log\rho}\left(\log\left|\rho^{n-m}\frac{\zeta}{\nu}\right|\right)^2 \\
&= \frac{(n-m)(n-m-1)}{2}\mathcal{A} - \frac{n-m}{2\pi}\log\left|\frac{\zeta}{\nu}\right| \\
&\quad + \frac{1}{2\pi}\log\left|P\left(\frac{\zeta}{\nu},\sqrt{\rho}\right)\right| + \frac{n-m}{2}\mathcal{A} \\
&\quad - \frac{1}{4\pi}\log\left|\frac{\zeta}{\nu}\right| - \frac{(n-m)^2}{2}\mathcal{A} + \frac{n-m}{2\pi}\log\left|\frac{\zeta}{\nu}\right| \\
&\quad + \frac{1}{4\pi\log\rho}\left(\log\left|\frac{\zeta}{\nu}\right|\right)^2 \\
&= G(\zeta,\nu;\overline{\zeta},\overline{\nu}).
\end{aligned}$$

References

[1] J.C. Mcwilliams, The emergence of isolated coherent vortices in turbulent flow, J. Fluid Mech. 146 (1984) 21–43.
[2] J. Jiménez, A. Guegan, Spontaneous generation of vortex crystals from forced two-dimensional homogeneous turbulence, Phys. Fluids 19 (8) (2007) 085103.
[3] C. Geldhauser, M. Romito, The point vortex model for the Euler equation, AIMS Math. 4 (3) (2019) 534–575, http://dx.doi.org/10.3934/math.2019.3.534.
[4] R.P. Feynman, Chapter II application of quantum mechanics to liquid helium, in: Progress in low temperature physics, Elsevier, 1955, pp. 17–53.
[5] V. Tkachenko, On vortex lattices, Sov. Phys. JETP 22 (6) (1966) 1282–1286.
[6] P.K. Newton, G. Chamoun, Vortex lattice theory: A particle interaction perspective, SIAM Rev. 51 (3) (2009) 501–542.
[7] R. Benzi, B. Legras, Wave-vortex dynamics, J. Phys. A: Math. Gen. 20 (15) (1987) 5125–5144.
[8] K.A. O'Neil, On the Hamiltonian dynamics of vortex lattices, J. Math. Phys. 30 (6) (1989) 1373–1379.
[9] K.A. O'Neil, Symmetric configurations of vortices, Phys. Lett. A 124 (9) (1987) 503–507, http://dx.doi.org/10.1016/0375-9601(87)90053-3.
[10] J.B. Weiss, J.C. McWilliams, Nonergodicity of point vortices, Phys. Fluids A: Fluid Dynamics 3 (5) (1991) 835–844.
[11] A.A. Kilin, E.M. Artemova, Integrability and chaos in vortex lattice dynamics, Regul. Chaotic Dyn. 24 (2019) 101–113.
[12] M. Abramowitz, I.A. Stegun (Eds.), Handbook of mathematical functions, Dover Books on Mathematics, Dover Publications, Mineola, NY, 1965.
[13] M. Stremler, H. Aref, Motion of three point vortices in a periodic parallelogram, J. Fluid Mech. 392 (1999) 101–128, http://dx.doi.org/10.1017/S002211209900542X.
[14] D. Crowdy, On rectangular vortex lattices, Appl. Math. Lett. 23 (1) (2010) 34–38.
[15] D. Crowdy, Solving Problems in Multiply Connected Domains, in: CBMS-NSF Regional Conference Series in Applied Mathematics, Society for Industrial & Applied Mathematics, New York, NY, 2020.
[16] M.A. Stremler, On relative equilibria and integrable dynamics of point vortices in periodic domains, Theor. Comput. Fluid Dyn. 24 (1–4) (2010) 25–37.
[17] K. Modin, M. Viviani, Integrability of point-vortex dynamics via symplectic reduction: A survey, Arnold Math. J. 7 (3) (2020) 357–385, http://dx.doi.org/10.1007/s40598-020-00162-8.
[18] C.C. Lin, On the motion of vortices in two dimensions: I. existence of the Kirchhoff-Routh function, Proc. Natl. Acad. Sci. USA 27 (12) (1941) 570–575.
[19] C.C. Lin, On the motion of vortices in two dimensions: II. Some further investigations on the Kirchhoff-Routh function, Proc. Natl. Acad. Sci. USA 27 (12) (1941) 575–577.
[20] P.K. Newton, The N-Vortex Problem: Analytical Techniques, in: Applied Mathematical Sciences, Springer New York, 2001, http://dx.doi.org/10.1007/978-1-4684-9290-3.
[21] C.C. Green, J.S. Marshall, Green's function for the Laplace–Beltrami operator on a toroidal surface, Proc. Roy. Soc. A 469 (2149) (2013) 20120479.
[22] T. Sakajo, Y. Shimizu, Point vortex interactions on a toroidal surface, Proc. Roy. Soc. A (2191) (2016) 20160271.
[23] T. Sakajo, Vortex crystals on the surface of a torus, Philos. Trans. Roy. Soc. A 377 (2158) (2019) 20180344.
[24] V.S. Krishnamurthy, M.H. Wheeler, D.G. Crowdy, A. Constantin, Steady point vortex pair in a field of Stuart-type vorticity, J. Fluid Mech. 874 (2019) R1, http://dx.doi.org/10.1017/jfm.2019.502.
[25] V.S. Krishnamurthy, M.H. Wheeler, D.G. Crowdy, A. Constantin, Liouville chains: new hybrid vortex equilibria of the two-dimensional Euler equation, J. Fluid Mech. 921 (2021) A1, http://dx.doi.org/10.1017/jfm.2021.285.
[26] T. Sakajo, V.S. Krishnamurthy, Quantized point vortex equilibria in a one-way interaction model with a Liouville-type background vorticity on a curved torus, J. Math. Phys. 63 (6) (2022) 063101, http://dx.doi.org/10.1063/5.0062659.
[27] B.N. Kuvshinov, T.J. Schep, Double-periodic arrays of vortices, Phys. Fluids 12 (12) (2000) 3282–3284, http://dx.doi.org/10.1063/1.1321262.
[28] K.A. O'Neil, Collapse of point vortex lattices, Physica D 37 (1–3) (1989) 531–538.
[29] N.J. Zabusky, M. Hughes, K. Roberts, Contour dynamics for the Euler equations in two dimensions, J. Comput. Phys. 30 (1) (1979) 96–106, http://dx.doi.org/10.1016/0021-9991(79)90089-5.
[30] D. Crowdy, A. Surana, Contour dynamics in complex domains, J. Fluid Mech. 593 (2007) 235–254, http://dx.doi.org/10.1017/s002211200700866x.
[31] D. Crowdy, The Schottky-Klein prime function on the Schottky double of planar domains, Comput. Methods Funct. Theory 10 (2) (2010) 501–517, http://dx.doi.org/10.1007/bf03321778.